PR12-18-001

Photoproduction of vector mesons on nuclei with GlueX

A. Ali,[10] M. Amaryan,[22] E. G. Anassontzis,[2] A. Austregesilo,[14] M. Baalouch,[22] F. Barbosa,[14] J. Barlow,[7] A. Barnes,[5] E. Barriga,[7] T. D. Beattie,[23] V. V. Berdnikov,[17] T. Black,[20] W. Boeglin,[6] M. Boer,[4] W. J. Briscoe,[8] T. Britton,[14] W. K. Brooks,[24] B. E. Cannon,[7] N. Cao,[13] E. Chudakov,[14] S. Cole,[1] J. Crafts,[19] V. Crede,[7] M. M. Dalton,[14] T. Daniels,[20] A. Deur,[14] S. Dobbs,[21] A. Dolgolenko,[12] M. Dugger,[1] R. Dzhygadlo,[10] H. Egiyan,[14] A. Ernst,[7] P. Eugenio,[7] C. Fanelli,[16] S. Fegan,[8] A. M. Foda,[23] J. Foote,[11] J. Frye,[11] S. Furletov,[14] L. Gan (spokesperson),[20] A. Gasparian (spokesperson),[19] N. Gevorgyan,[27] C. Gleason,[11] K. Goetzen,[10] A. Goncalves,[7] V. S. Goryachev,[12] L. Guo,[6] H. Hakobyan,[24] A. Hamdi,[10] S. Han,[30] J. Hardin,[16] G. M. Huber,[23] A. Hurley,[29] D. G. Ireland,[9] M. M. Ito,[14] N. S. Jarvis,[3] R. T. Jones,[5] V. Kakoyan,[27] G. Kalicy,[4] M. Kamel,[6] C. Kourkoumeli,[2] S. Kuleshov,[24] I. Larin (spokesperson),[15,12] D. Lawrence,[14] D. Lersch,[7] M. Levillain,[19] H. Li,[3] W. Li,[29] B. Liu,[13] K. Livingston,[9] G. J. Lolos,[23] V. Lyubovitskij,[25,26] D. Mack,[14] H. Marukyan,[27] P. T. Mattione,[14] V. Matveev,[12] M. McCaughan,[14] M. McCracken,[3] W. McGinley,[3] J. McIntyre,[5] C. A. Meyer,[3] R. Miskimen,[15] R. E. Mitchell,[11] F. Mokaya,[5] F. Nerling,[10] A. I. Ostrovidov,[7] Z. Papandreou,[23] M. Patsyuk,[16] P. Pauli,[9] R. Pedroni,[19] L. Pentchev,[14] K. J. Peters,[10] W. Phelps,[6] E. Pooser,[14] N. Qin,[30] J. Reinhold,[6] B. G. Ritchie,[1] L. Robison,[21] D. Romanov,[17] C. Romero,[24] C. Salgado,[18] R. A. Schumacher,[3] A. Schertz,[29] C. Schwarz,[10] J. Schwiening,[10] K. K. Seth,[21] X. Shen,[13] M. R. Shepherd,[11] E. S. Smith,[14] D. I. Sober,[4] A. Somov (spokesperson, contact person),[14] S. Somov,[17] O. Soto,[24] M. J. Staib,[3] J. R. Stevens,[29] I. I. Strakovsky,[8] V. Tarasov,[12] S. Taylor,[14] A. Teymurazyan,[23] G. Vasileiadis,[2] D. Werthmüller,[9] T. Whitlatch,[14] N. Wickramaarachchi,[22] M. Williams,[16] T. Xiao,[21] Y. Yang,[16] J. Zarling,[11] Z. Zhang,[30] G. Zhao,[13] Q. Zhou,[13] X. Zhou,[30] and B. Zihlmann[14]

[1] *Arizona State University, Tempe, Arizona 85287, USA*

[2] *National and Kapodistrian University of Athens, 15771 Athens, Greece*

[3] *Carnegie Mellon University, Pittsburgh, Pennsylvania 15213, USA*

[4] *Catholic University of America, Washington, D.C. 20064, USA*

[5]*University of Connecticut, Storrs, Connecticut 06269, USA*

[6]*Florida International University, Miami, Florida 33199, USA*

[7]*Florida State University, Tallahassee, Florida 32306, USA*

[8]*The George Washington University, Washington, D.C. 20052, USA*

[9]*University of Glasgow, Glasgow G12 8QQ, United Kingdom*

[10]*GSI Helmholtzzentrum für Schwerionenforschung GmbH, D-64291 Darmstadt, Germany*

[11]*Indiana University, Bloomington, Indiana 47405, USA*

[12]*Institute for Theoretical and Experimental Physics, Moscow 117259, Russia*

[13]*Institute of High Energy Physics, Chinese Academy of Science,*
Shijingshan, Beijing 100049, People's Republic of China

[14]*Thomas Jefferson National Accelerator Facility, Newport News, Virginia 23606, USA*

[15]*University of Massachusetts, Amherst, Massachusetts 01003, USA*

[16]*Massachusetts Institute of Technology,*
Cambridge, Massachusetts 02139, USA

[17]*National Research Nuclear University Moscow*
Engineering Physics Institute, Moscow 115409, Russia

[18]*Norfolk State University, Norfolk, Virginia 23504, USA*

[19]*North Carolina A&T State University,*
Greensboro, North Carolina 27411, USA

[20]*University of North Carolina at Wilmington,*
Wilmington, North Carolina 28403, USA

[21]*Northwestern University, Evanston, Illinois 60208, USA*

[22]*Old Dominion University, Norfolk, Virginia 23529, USA*

[23]*University of Regina, Regina, Saskatchewan, Canada S4S 0A2*

[24]*Universidad Técnica Federico Santa María, Casilla 110-V Valparaíso, Chile*

[25]*Tomsk State University, 634050 Tomsk, Russia*

[26]*Tomsk Polytechnic University, 634050 Tomsk, Russia*

[27]*A. I. Alikhanian National Science Laboratory (Yerevan Physics Institute), 0036 Yerevan, Armenia*

[28]*Joint Institute for Nuclear Research, 141980 Dubna, Moscow region, Russia*

[29]*College of William and Mary, Williamsburg, Virginia 23185, USA*

[30]*Wuhan University, Wuhan, Hubei 430072, People's Republic of China*

Contents

Abstract

We propose to measure the photoproduction cross sections and the spin density matrix elements (ρ^A_{00}) of vector mesons ρ, ω, and ϕ on four nuclear targets (^{12}C, ^{28}Si, ^{120}Sn, and ^{208}Pb) in the photon beam energy range of 6–12 GeV with the GlueX apparatus. The nuclear transparency ($A_{eff} = \sigma_A/\sigma_N$) for these mesons over a wide beam energy range will be extracted by normalizing the measured nuclear cross sections to the corresponding cross sections on the hydrogen target from the GlueX experiment. The previous experimental result from the ρ meson photoproduction shows nearly no beam energy dependence for the nuclear transparency, which is in contradiction to the theoretical predictions. The proposed measurement of A_{eff} over a wide beam energy range will help to resolve this discrepancy. In addition, the measured nuclear transparency (A_{eff}) and the spin density matrix element (ρ^A_{00}) for ω mesons will offer two independent ways to extract the cross section of the longitudinally polarized ω mesons on nucleon ($\sigma_L = \sigma(\omega_L N)$) for the first time. This will provide critical information for understanding the color transparency effect in the electroproduction of vector mesons.

I. RESPONSE TO PAC45 REPORT

PR12-17-010

Scientific Rating: N/A

Recommendation: deferred

Title: Photoproduction of vector mesons on nuclei with GlueX

Spokespersons: Liping Gan, Ashot Gasparian, Ilya Larin, Alexander Somov (Contact), Sergey Gevorkyan

Motivation: The proposed measurements aim to study the photoproduction of light vector mesons on nuclear targets with photon beam energies between 6 and 12 GeV using the GlueX detector. The primary focus is on the first extraction of the cross-section of longitudinally polarized ω on nucleons $\sigma_L(\omega N)$ from incoherent photoproduction off nuclear targets (C, Si, Sn and Pb). Two methods to access the $\sigma_L(\omega N)$ are proposed: the measurement of nuclear transparency $A_{eff}=\sigma_A/A\sigma_N$ and the spin density matrix element ρ_{00}. The measurements of the nuclear absorption in different nuclei are useful for extracting meson-nucleon cross sections while the use of different beam energies will shed light on the disagreement between earlier experimental results and existing theory predictions and provide additional information on color transparency. The proposed measurements provide a unique opportunity to access $\sigma_L(\omega N)$ and when combined with the already known cross section for transverse polarization $\sigma_T(\omega N)$ would give important information on the dependence of the vector meson – nucleon interaction on the polarization.

Measurement and Feasibility: The proposed experiment would utilize the standard GlueX detector package. The collaboration's extensive experience in reconstructing multi-particle π^0 and photon final states should make reconstruction of the vector mesons straightforward. However, the proposal lacks critical details about the methods that will be used to measure the nuclear transparency and to extract the meson-nucleon cross section. As a result it is not possible to verify the stated systematic errors and confirm the beam time estimates.

Issues: While a first measurement of $\sigma_L(\omega N)$ is compelling, the connection to theoretical models needs to be strengthened. It is not clear from the proposal how the measurement of $\sigma_L(\omega N)$ will aid in the "interpretation of color transparency effects in the electroproduction of vector mesons".

Summary: The PAC considers the proposed measurements and in particular the extraction of $\sigma_L(\omega N)$ interesting and encourages the collaboration to better spell out the experimental technique to be used.

The experimental similarities with the proposal PR12-17-007 must be studied in detail to hopefully overcome their differences and settle on a common beam time request.

PAC45 comment: The proposed experiment would utilize the standard GlueX detector package. The collaboration's extensive experience in reconstructing multi-particle and photon final states should make reconstruction of the vector mesons straightforward. However, the proposal lacks critical details about the methods that will be used to measure the nuclear transparency and to extract the meson-nucleon cross section. As a result it is not possible to verify the stated systematic errors and confirm the beam time estimates.

In the proposed experiment we will measure the photoproduction cross sections (σ_A) and the spin density matrix elements (ρ^A_{00}) of vector mesons on four nuclear targets in the beam energy range between 6 GeV and 12 GeV. The nuclear transparency ($A_{eff} = \sigma_A/\sigma_N$ [1]) will be obtained by calculating the ratio of the measured nuclear cross section to the cross section on a free proton from the existing GlueX data. The spin density matrix element ρ^A_{00} will be extracted from a fit to the angular distribution of a vector meson decay in the helicity frame as described in Section X.B. Both the nuclear transparency A_{eff} and the spin density matrix element ρ^A_{00} are related to the interaction cross section of longitudinally polarized ω mesons with nucleon $\sigma_L(\omega_L N)$, as discussed in Section V.B. The cross section $\sigma_L(\omega_L N)$ can be extracted from the measured A_{eff} or ρ^A_{00} using theoretical predictions.

Several new sections are added in the proposal to provide more detail. The reconstruction of ω, ρ, and ϕ mesons with the GlueX detector using Monte Carlo simulation is described in Section VI. We also studied the experimental capabilities of reconstructing the vector mesons on nuclear targets by analyzing the existing empty target data from the GlueX experiment, where mesons were produced on the target walls. The result of this study is discussed in Section VII. The production rate and the expected number of reconstructed mesons for the proposed experiment are presented in Section IX. Statistical and systematic uncertainties on the measurements of A_{eff} and ρ^A_{00}, and uncertainties on the cross section σ_L extracted from these measurements are given in Section X

PAC45 comment: While a first measurement of $\sigma_L(\omega N)$ is compelling, the connection to theoretical models needs to be strengthened. It is not clear from the proposal how the measurement of σ_L will aid in the interpretation of color transparency effects in the electroproduction of vector mesons.

The connection of σ_L to the theoretical models is discussed in Section II.B.

QCD predicts that hadrons produced in exclusive reactions with sufficiently high squared four momentum transfer (Q^2) will have significantly less interactions with nuclei due to the reduced transverse size of hadrons $r_T \sim 1/Q$. This is called color transparency (CT). As a result, the nuclear transparency, defined as the ratio of nuclear cross section to that on a free nucleon,

[1] In literature, the nuclear transparency is usually defined as the ratio of the cross section per target nucleon $T = \sigma_A/A\,\sigma_N$. In the text we also refer A_{eff} to as a nuclear transparency.

will increase as Q^2 increases due to less attenuation for the out-going mesons to propagate through a nucleus. On the other hand, the fraction of longitudinally polarized vector mesons grows with Q^2 as observed in the previous experiment [4] and is shown in the right plot of Fig. 3. If the meson-nucleon cross section depends on the polarization, and if $(\sigma_T(\rho N) > \sigma_L(\rho N))$, then the out-going mesons will have less absorption in the nuclear media due to growing number of the longitudinally polarized mesons at higher Q^2. This will increase the nuclear transparency as Q^2 increases. There is similar effect for CT. Recent theoretical calculations of the nuclear transparency computed for $\sigma_L = 10$ mb (and $\sigma_T = 26$ mb), predicted by the ADC/QCD holographic wave function of ρ meson are shown as magenta stars on the nuclear transparency measurements of the CLAS collaboration, shown on the left plot of Fig 3. As one can see, this effect accounts for about 20% of the total increase of the nuclear transparency for ^{56}Fe. In order to extract the color transparency from the observed nuclear transparency shown in Fig 3, it is clear that one has to separate these two effects. The knowledge of σ_L is important for the interpretation of the color transparency effect in the electroproduction of vector mesons.

PAC45 comment: The experimental similarities with the proposal PR12-17-007 must be studied in detail to hopefully overcome their differences and settle on a common beam time request.

The proposal PR12-17-007 is not planned to be resubmitted to this PAC. We believe that data collected by the proposed experiment will be valuable for PR12-17-007 if it is submitted to a future PAC.

We would also like to point out that the run conditions for this proposed experiment are rather different from PR12-17-007. In order to study beam energy dependence of the nuclear transparency, we require a wide beam energy range of 6–12 GeV and an additional two heavy targets, ^{120}Sn and ^{208}Pb. Therefore, the experiment has to run at a relatively small luminosity in order to provide clean reconstruction of mesons. On the other hand, due to the relatively small cross sections for the reactions on lighter nuclear targets proposed by PR12-17-007, the experiment has to operate at higher luminosity. The event reconstruction will be performed in a small beam energy range of 8–9 GeV because of a large fraction of accidental hits in the tagging detectors.

II. INTRODUCTION

We propose to study the photoproduction of light vector mesons with the GlueX detector using a set of nuclear targets: ^{12}C, ^{28}Si, ^{120}Sn, and ^{208}Pb in a wide beam energy range from 6 GeV to 12 GeV. The nuclear transparency ($A_{eff} = \frac{\sigma_A}{\sigma_N}$, where σ_A and σ_N are production cross sections on nuclei and free nucleon, respectively) and the spin density matrix element (ρ^A_{00}) of these mesons will be extracted. The primary goal of the experiment is as following:

- Measure the beam energy dependency of the nuclear transparency of light vector mesons to resolve the disagreement between the theoretical predictions [5, 6] and the experimental results [7–9]. As shown in Fig. 1, the decrease of nuclear transparency with the beam energy predicted by theory [6] was not observed in ρ [7] photoproduction. Similar situations are for $\pi^{\pm}, \pi^0$ photoproduction [8, 9] as well. Understanding this discrepancy is fundamental for nuclear physics.

- Independently extract the longitudinally polarized ω-nucleon cross section ($\sigma_L(\omega_L N)$) from two different observables to provide critical information for understanding of color transparency effect in the electroproduction of vector mesons: (1) the nuclear transparency (A_{eff}) and (2) the spin density element (ρ^A_{00}).

III. PHYSICS MOTIVATION

A. Energy dependence of the nuclear transparency

Measurements of A-dependence of the nuclear transparency of vector mesons at different energies relevant to GlueX are important because they will provide information related to the long standing problem: weak energy dependence of the nuclear transparency measured for ρ mesons at Cornel [7], which contradicts theoretical predictions [6]. The nuclear transparency measured at two photon energies $E_\gamma = 4$ GeV and $E_\gamma = 8$ GeV is shown in Fig. 1. In this figure, the nuclear transparency is defined as $A_{eff} = \sigma_A/\sigma_N$, where σ_A and σ_N are photoproduction cross sections on nuclei and nucleon, respectively. Hereafter we will follow this definition. The transparencies are similar for these energies within the errors limit unlike the theoretical calculations [6], which predict the significant decrease of the transparency with energy due

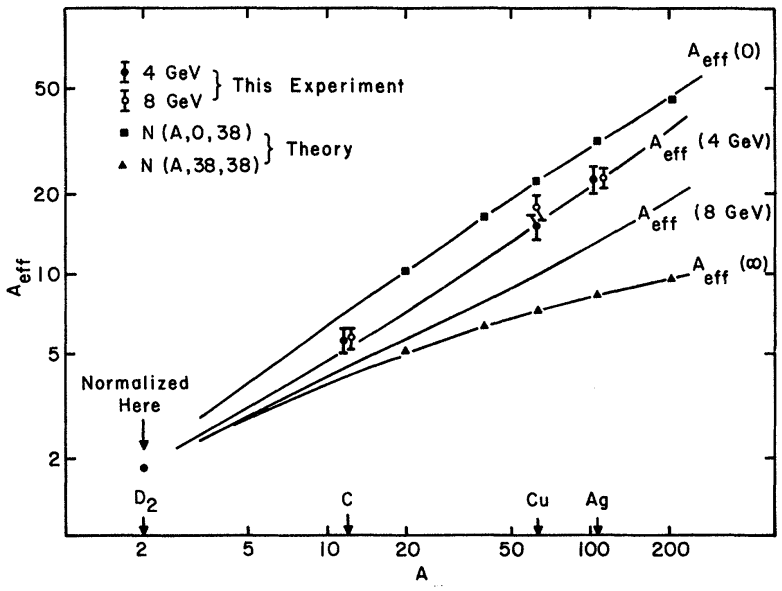

FIG. 1: Nuclear transparency for incoherent photoproduction of ρ mesons at $\mid t \mid = 0.1$ GeV^2 and different energies [7].

to the impact of the energy-dependent coherence length $\tau_c = \frac{1}{q_L} = \frac{2E_\gamma}{m_V^2}$ on the incoherent photoproduction.

B. Dependence of vector particle interactions on polarization

For particles with nonzero spin, such as vector mesons V (ρ, ω, ϕ), interactions with nucleons are represented by a set of polarization-dependent amplitudes and can result in different cross sections for transversely and longitudinally polarized vector mesons with nucleons. The meson-nucleon cross sections can be extracted by measuring the absorption of mesons in production off nuclei.

The first indication that interaction of a vector mesons V (ρ, ω, ϕ) with a nucleon depends on the meson polarization comes from the ρ electroproduction data. The ratio of production cross sections for a proton target can be represented as $R = \sigma(\gamma_L p \to \rho p)/\sigma(\gamma_T p \to \rho p) = \xi^2 \frac{Q^2}{m_\rho^2}$, where the parameter ξ corresponds to the ratio of the longitudinal to transverse ρ^0 total cross sections $\xi = \sigma_L(\rho p)/\sigma_T(\rho p)$. The value of ξ obtained from measurements is $\xi \approx 0.7$ [10], while the naive quark model predicts equal cross sections $\sigma_L(\rho p) = \sigma_T(\rho p)$. In the case of ϕ electroproduction [11] this ratio is $\xi \approx 0.6$. Some interpretations of the deep inelastic scattering

data using the generalized vector dominance model [12] also allow for the large difference between $\sigma_L(Vp)$ and $\sigma_T(Vp)$ ($\xi \approx 0.25$).

The dependence of vector particle interactions on the particle's polarization has been known for many years in the case when the constituents of the particle are in the D-wave state. A good example of such effect is the deuteron interaction with matter [13]. The D-wave component in the deuteron wave function leads to different absorption in matter for transversely and longitudinally polarized deuterons. This effect was experimentally measured in Dubna [14] and Juelich [15]. There are also predictions that the interaction of mesons with nonzero orbital momentum with nucleons is strongly correlated with the meson polarization [16, 17]. For the ground-state S-wave vector mesons (ρ, ω, ϕ) the D-wave component in their wave functions can emerge as a result of the Lorentz transformation [18]. The origin of a difference between $\sigma_T(VN)$ and $\sigma_L(VN)$ explained by the appearance of a D-wave contribution in the vector meson wave function in the infinite momentum frame.

The only attempt to study the impact of the vector meson polarization on its absorption was made many years ago at ITEP [19] using the charge exchange reaction $\pi^- + A \to \rho^0 + A'$. The incoherent cross section and polarization of ρ mesons were measured on a set of different nuclei: C, Al, Cu, Pb. Due to the dominance of the pion exchange in this process a large fraction of longitudinally polarized ρ mesons was produced. At first glance the experimental data supported the assumption that $\sigma_T(\rho N) = \sigma_L(\rho N)$. However, there are reasons against such a conclusion. It was shown [20] that due to the low energy of the primary beam (E_π = 3.7 GeV) and the large decay width of the ρ meson some mesons decay inside the nucleus, which complicates the interpretation of the experimental data.

The total cross sections of ρ and $f(1270)$ mesons with a nucleon were measured at Argonne [21] using the charge exchange process on neon nuclei $\pi^+ + Ne \to \rho(f) + Ne'$. In order to account for decays of the ρ mesons in nuclei (p_π = 3.5 GeV/c) the total cross section is required to be $\sigma(\rho N) \approx 12$ mb, which contradicts to the value $\sigma(\rho N) \approx 27$ mb obtained from the ρ meson photoproduction on nuclei. From our point of view this difference is a result of distinction between $\sigma_T(\rho N)$ and $\sigma_L(\rho N)$. In the charge exchange process mainly longitudinally polarized ρ mesons are produced, whereas in the photoproduction ρ mesons are transversely polarized.

According to measurements at SLAC [2], in the kinematic region of the proposed experiment with a modest momentum transfer, longitudinally polarized vector mesons will be produced

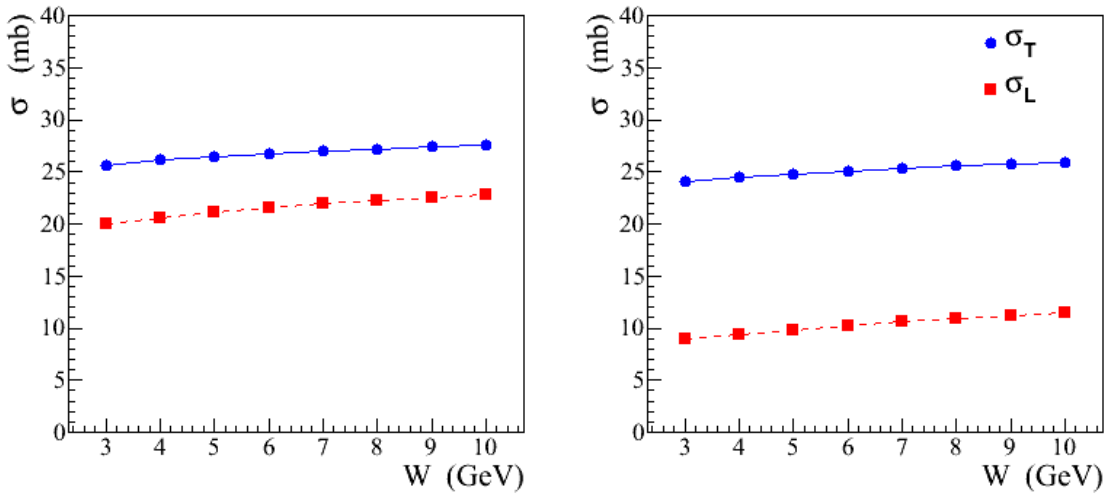

FIG. 2: Energy dependence of the total cross sections $\sigma_L(\rho N)$ and $\sigma_T(\rho N)$ computed for different ρ meson wave functions: boosted gaussian wave function [28] (left) and ADC/QCD holographic [29] wave function [30, 31](right).

through pion exchange process. While the total cross section for interaction of the transversely polarized vector meson with nucleon ($\sigma_T = \sigma(V_T N)$) can be measured from the coherent photoproduction; the meson photoproduction in the incoherent region provides a unique opportunity to extract the yet unmeasured total cross section for longitudinally polarized vector mesons $\sigma_L = \sigma((V_L N)$. Compared to the electroproduction, production of ω by real photons has certain advantages to study meson absorption in a nucleus. In the real photoproduction at modest transfer momenta $\mid t \mid \leq 1$ GeV^2, the color transparency effect is absent. The reduced absorption with $\mid t \mid$ will solely be a result of the difference between σ_T and σ_L.

C. Theoretical predictions for $\sigma_L(VN)$ and $\sigma_T(VN)$

The total cross sections $\sigma_T(VN)$ and $\sigma_L(VN)$ can be calculated in the framework of the color dipole model [25, 26]. The dependence of $\sigma_L(\rho N)$ and $\sigma_T(\rho N)$ on the energy $W = \sqrt{s}$ computed for different choices of the ρ meson wave functions is shown in Fig. 2 [27]. The cross sections obtained for the boosted gaussian wave function [28] are shown on the left plot and ADC/QCD holographic [29] wave function [30, 31] are presented on the right plot. The cross section $\sigma_L(\rho N)$ is predicted to be smaller than $\sigma_T(\rho N)$ for both wave functions.

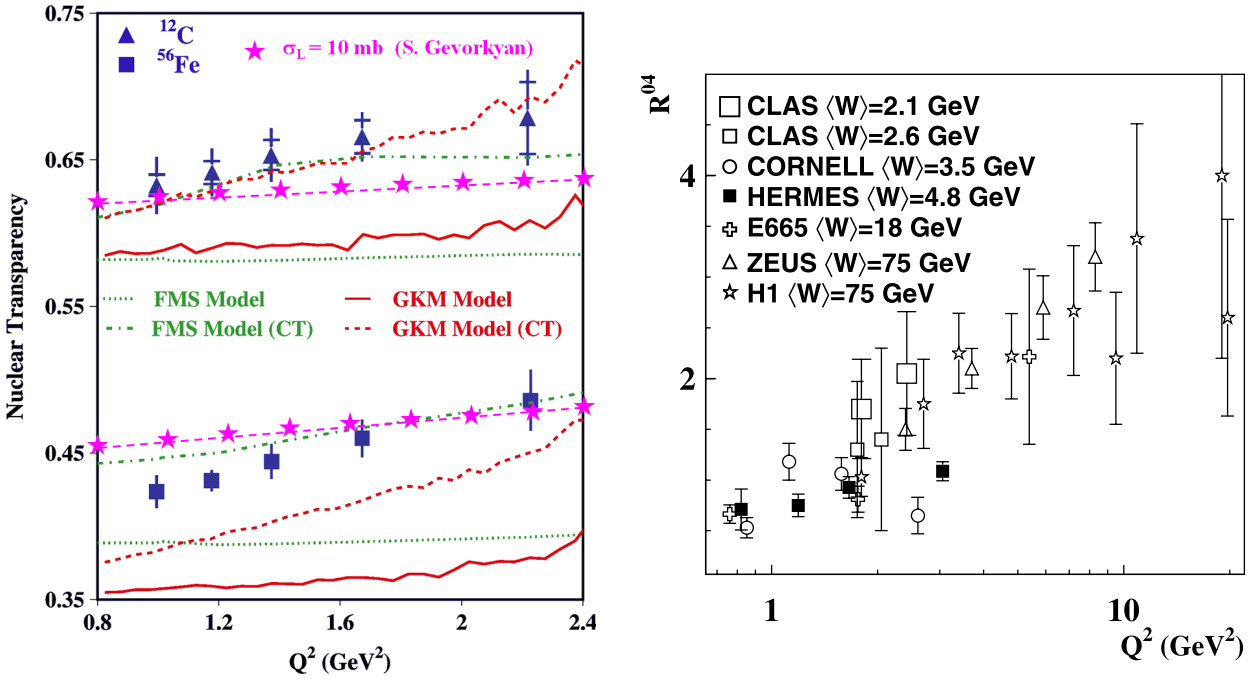

FIG. 3: Nuclear transparency as a function of Q^2. Experimental data are from CLAS, JLab [24] (left). Q^2 dependence of the ratio of the longitudinal-to-transverse cross sections for exclusive ρ^0 production on proton [4] (right). Recent theoretical calculations of the nuclear transparency performed for $\sigma_L = 10$ mb and $\sigma_T = 26$ mb, predicted by the ADC/QCD holographic wave function of ρ meson [30, 31](stars on the left plot).

D. Impact of $\sigma_L(VN)$ on the color transparency

The knowledge of the cross section $\sigma_L(VN)$ is important for interpreting the color screening effect in leptoproduction [22]. The idea of the color transparency (CT) is that an object (hadron) produced in certain hard-scattering processes has a smaller probability to interact in the nuclear matter due to its smaller size compared with the physical hadron. As a result, the color transparency increases the nuclear transparency. On the other hand, the nuclear transparency depends on the values of $\sigma_L(VN)$ and $\sigma_T(VN)$. Fig. 3 represents the dependence of the nuclear transparency in the ρ meson electroproduction as a function of the virtuality of the photon Q^2 measured by the CLAS experiment. The ρ meson absorption in nuclei decreases with the increase of the Q^2, which is accounted for the CT effect. At the same time, the fraction of longitudinally polarized vector mesons also grows at large Q^2 as shown on the right plot of Fig. 3. If we assume that $\sigma_T(VN) > \sigma_L(VN)$, the effect of the absorption weakening at large

Q^2 cannot be entirely described by the CT; differences between interactions of longitudinally and transversely polarized vector mesons with nucleon have to be considered.

Recent theoretical predictions [22] of the dependence of the nuclear transparency dependence on Q^2 due to the different values of $\sigma_{L,T}$ are presented as stars on the left plot of Fig. 3. The nuclear transparency was computed according to equations described in Section 5.B and using ρ-nucleon cross sections $\sigma_L = 10$ mb and $\sigma_T = 26$ mb. These cross sections are predicted by the ADC/QCD holographic wave function of ρ meson [30, 31] The decrease of the nuclear transparency for the ^{56}Fe data due to different values of $\sigma_{L,T}$ is estimated to be about 5.5% and constinutes to $\sim 25\%$ of the total decrease of the measured nuclear transparency at large Q^2.

Measurements of the proposed experiment at GlueX will be used to extract the value of σ_L and constrain the contribution to the nuclear transparency from different $\sigma_{L,T}$, which is important for the interpretation of the color screening effect.

E. Why ω mesons ?

Study photoproduction of ω mesons on different nuclei and beam energies provides a unique opportunity to measure energy dependence of the nuclear transparency predicted by theoretical models [1] and extract the total cross section of longitudinally polarized mesons with nucleon $\sigma_L = \sigma(\omega N)$. Unlike ρ and ϕ mesons, which due to the s-channel helicity conservation in photoproduction are produced mainly transversely polarized, the pion exchange in the ω meson photoproduction leads to the noticeable production of longitudinally polarized ω mesons [2]. The dependence of the spin density matrix elements on the invariant momenta transfer in the process $\gamma + p \rightarrow \omega + p$ measured by SLAC [2] is presented in Fig. 4. The fraction of the longitudinally polarized ω mesons determined by the value of ρ_{00} is significant even at large beam energies of $E_\gamma = 10$ GeV. The total cross sections of longitudinally and transversely polarized mesons with nucleon $\sigma_{L,T} = \sigma(\omega N)$ can be obtained from the incoherent and coherent photoproduction, respectively.

IV. PHOTOPRODUCTION OF ω MESONS ON NUCLEI

In the late 60's and early 70's many experiments were carried out to study vector mesons photoproduction on nuclei [5]. These experiments had two main goals:

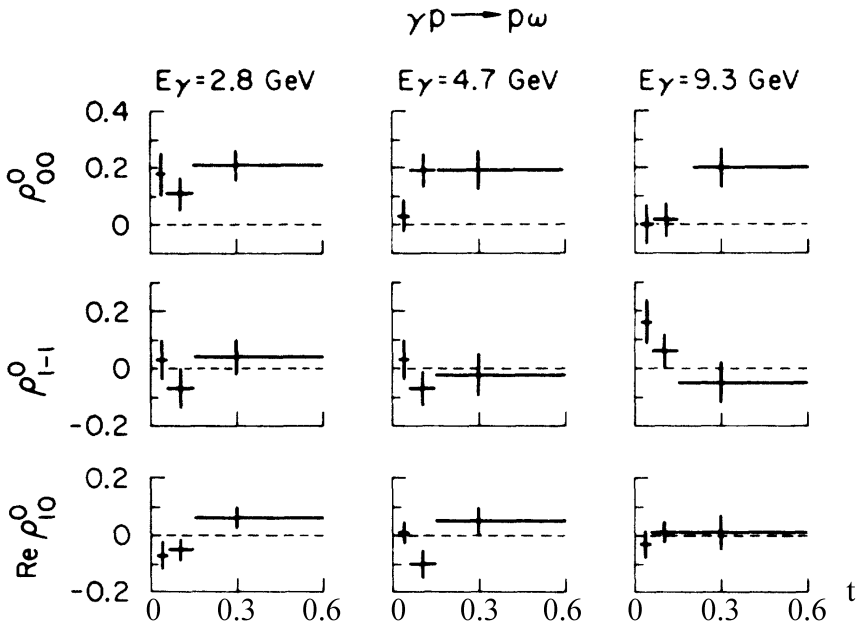

FIG. 4: Spin density matrix elements of ω mesons in the helicity system measured by the SLAC experiment [2].

- Extraction of vector meson-nucleon total cross sections $\sigma(VN)$ in order to check quark model predictions.

- Verification of the vector dominance model (VDM) and finding the limits of its validity.

The first ω photoproduction experiments at high energies using a large set of nuclei were carried out by the Rochester group at Cornell [32, 33] and the Bonn-Pisa group at DESY [34]. The mean photon energies used at Cornell were 6.8 GeV and 9.0 GeV. The ω mesons were detected via the 3π decay mode. The Bonn-Pisa group used beam photons with a mean energy of 5.7 GeV. The ω mesons were reconstructed using the $\pi^0\gamma$ decay mode. Both experiments confirmed the naive quark model prediction: $\sigma(\omega N) = \sigma(\rho N) = (\sigma(\pi^+ N)+\sigma(\pi^- N))/2$. A later experiment on ω photoproduction off nuclei at a mean energy of 3.9 GeV was performed at the electron synchrotron NINA at Daresburry [35]. The nuclear absorption of ω mesons was found to be in agreement with the previous experiments. The total cross section $\sigma(\omega N)$ was extracted from the coherent part of the photoproduction cross section, whereas the incoherent part was considered to be an undesirable background. Experiments confirmed quark model predictions for total cross section of vector mesons interaction with nucleon, which is not strange because from the coherent part of the cross section one extracts [1] only cross section of the transversely

polarized mesons, $\sigma_T(\omega N)$.

Recently, the omega mesons photoproduction was measured by CBELSA/TAPS [36] collaboration via the decay $\omega \to \pi^0\gamma$ and at by the CLAS collaboration at Jefferson Lab [37] using the rare electromagnetic decay mode $\omega \to e^+e^-$. The main goal was to investigate the impact of the nuclear environment on the vector mesons mass and decay width. In order to have a significant fraction of the ω mesons decay in the nuclei, the mesons momentum in both experiments was low ($p_\omega \geq 0.8$ GeV in CLAS experiment and $p_\omega \geq 0.2$ GeV in CBELSA/TAPS experiment). At such low momenta the large contribution from nucleon resonances complicates the interpretation of experimental results [39].

The CLAS collaboration observed a significantly stronger absorption of the ω meson than measured by the CBELSA/TAPS collaboration[2]. Both experiments obtained a relatively large in-medium width of ω mesons and $\sigma(\omega N)$ total cross section, which disagrees with measurements of the KEK-E325 experiment [40], where ω mesons were produced using a 12 GeV proton beam. The KEK-E325 collaboration also reported the ω-meson mass shift, which is not confirmed by the CBELSA/TAPS and E01-112 experiments. Disagreements between the experimental measurements are not fully understood up to now.

In all these experiments no attempt was done to separate the absorption of transversely and longitudinally polarized omega mesons. This effect can potentially be studied using the GlueX detector in Hall D, the new experimental facility constructed at Jefferson Lab. The Hall D facility provides a photon beam produced by 12 GeV electrons using the bremsstrahlung process. The experiment will allow to study photoproduction of mesons by reconstructing both neutral and charged final states in the beam energy range between 5 GeV and 12 GeV.

Photoproduction of ω mesons on nuclear targets in the GlueX kinematic region is a unique way to study the dependence of the strong interaction on the polarization of vector mesons. The reasons look as follows:

- Photoproduction of ω mesons on nucleons $\gamma N \to \omega N$ at the photon energies of several GeV is dominated by t-channel Pomeron exchange (diffraction, natural parity exchange) and one-pion-exchange (unnatural parity exchange). The pion exchange leads to production of longitudinally polarized ω mesons, unlike the diffraction process, which results in

[2] In the first paper [36] the CBELSA/TAPS collaboration published the cross section $\sigma(\omega N) = 70$ mb, recently [38] the cross section is corrected to the much lower value.

the production of transversely polarized mesons due to s-channel helicity conservation. The contributions from the diffraction and pion exchange are almost equal at a photon energy of $E_\gamma = 5$ GeV [5]. Measuring the ω meson production at different energies would provide data samples with different contributions of the longitudinally polarized ω mesons.

- In the coherent photoproduction the unnatural exchange part of the elementary amplitude cancels out since in the coherent processes the amplitudes for interactions with protons and neutrons are added with the opposite signs. Therefore, from the coherent photoproduction one can extract only the total cross section of transversely polarized vector mesons on nucleons [1].

- In the incoherent photoproduction the cross section on the nucleus is the sum of the photoproduction cross sections on individual nucleons. As a result ω mesons with both polarizations can be produced. This can be used to study the interaction of longitudinally polarized vector mesons with the matter [1].

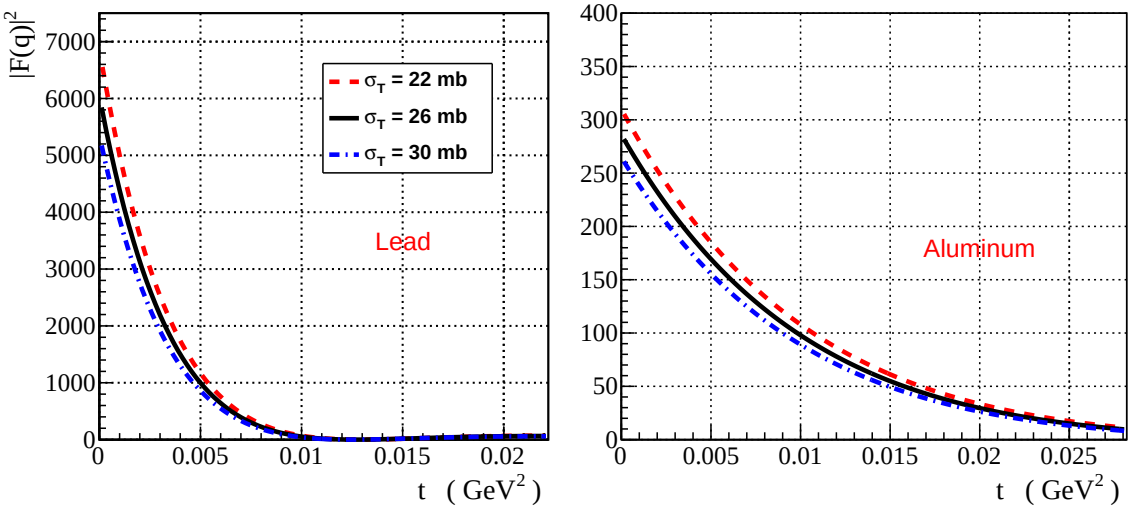

FIG. 5: Dependence of the nuclear form factors on the invariant transfer momentum for different cross sections of transversely polarized ω mesons with nucleons.

V. THEORETICAL PREDICTIONS OF NUCLEAR CROSS SECTIONS

A. Coherent photoproduction

The differential cross section of coherent photoproduction of ω (nuclear target remains in the ground state) $\gamma + A \to \omega + A$ reads [1, 5]:

$$\frac{d\sigma}{dt} = \frac{d\sigma_N(0)}{dt} \mid F_A(q_L, q, \sigma_T) \mid^2, \tag{1}$$

where $\frac{d\sigma_N(0)}{dt}$ is the diffractive part of the forward cross section on the nucleon $\gamma(k) + N \to \omega(p) + N$, and $F_A(q_L, q, \sigma_T)$ is the nucleus form factor, which accounts for the ω absorption in nucleus. The form factor depends on the photon energy through the longitudinal momentum transferred $q_L = \frac{m_\omega^2}{2k}$. The two dimensional transverse momentum $\vec{q}$ is given by the standard relation $\vec{q}^2 = 4kpsin^2\frac{\theta}{2}$, thus the invariant transfer momenta: $t = (k-p)^2 = -q_L^2 - q^2$. In the coherent photoproduction, where one has to sum the elementary amplitude from different nucleons, the part of photoproduction amplitude on nucleon relevant to one pion exchange has a different signs for photoproduction on proton and neutron. This leads to cancellation of one pion exchange part[3] and to production of only transversely polarized ω mesons in coherent photoproduction on nuclei [1]. Figure 5 shows the dependence of the form factor on the transfer momentum for two nuclei and different values of $\sigma_T(\omega N)$.

B. Incoherent photoproduction

We propose to study two main physics topics using incoherent photoproduction of vector mesons:

- measure energy dependence of the nuclear transparency of vector mesons,
- measure the nuclear transparency and spin density matrix elements for ω mesons with the aim to extract the yet unmeasured cross section of longitudinally polarized ω mesons with nucleons.

Especially interesting are measurements of the incoherent photoproduction of ω mesons on a set of nuclei [1]. Unlike the coherent photoproduction from which one can extract only the

[3] Strictly speaking this is true only for symmetric nuclei. In the case of nuclei with unequal numbers of protons and neutrons, relevant corrections have be taken into account in a known way.

value of the transverse cross section $\sigma_T(\omega N)$, measuring ω cross section and spin density matrix elements on nuclei in the incoherent photoproduction allows one to determine the value of unknown longitudinal cross section $\sigma_L(\omega N)$. The incoherent part of the photoproduction cross section of ω mesons in the typical range of the momentum transfer 0.1 GeV^2 $< t <$ 0.5 GeV^2 can be presented in the following form [1]:

$$\begin{aligned}
\frac{d\sigma_A(q)}{dt} &= \frac{d\sigma_0(q)}{dt}(\rho_{00}N(0,\sigma_L) + (1-\rho_{00})N(k,\sigma_T)) \\
N(0,\sigma) &= \int \frac{1-\exp(-\sigma\int\rho(b,z)dz)}{\sigma}d^2b \\
N(k,\sigma) &= \int \rho(b,z) \mid E(b,z) \mid^2 dz d^2b \\
E(b,z) &= \exp(-\frac{\sigma}{2}\int_z \rho(b,z')dz') - \frac{\sigma}{2}\int^z \rho(b,z')dz' e^{iq_L(z'-z)} \exp(-\frac{\sigma}{2}\int_{z'}\rho(b,z'')dz'') \qquad (2)
\end{aligned}$$

Here $\rho(r)$ is the nuclear density;$\frac{d\sigma_0(q)}{dt} = \frac{d\sigma_N(q)}{dt} + \frac{d\sigma_U(q)}{dt}$ is the differential cross section of ω meson photoproduction on nucleon, which accounts for diffraction and unnatural parity exchanges; ρ_{00} is the spin density matrix element in the helicity system, relevant to the fraction of longitudinally polarized mesons in photoproduction on nucleon. The spin density matrix elements in photoproduction on nuclei and nucleons can be related as follows [1]:

$$\rho_{00}^A = \frac{N(0,\sigma_L)}{\rho_{00}N(0,\sigma_L) + (1-\rho_{00})N(k,\sigma_T)}\rho_{00} \qquad (3)$$

In Fig. 6 and 7 we present the A-dependence of the nuclear transparency A_{eff} and the spin density matrix element ρ_{00}^A calculated according to Eq. (2) and (3) for two energies and three values of σ_L. Fig. 8 demonstrates our predictions for the dependence of A_{eff} and ρ_{00}^A on σ_L for lead nuclei. The input values of $\rho_{00} = 0.2$ and total transverse ω-nucleon cross section [34] $\sigma_T(\omega N) = 26$ mb are taken from SLAC measurements [2].

Predicted energy dependence of the nuclear transparency for ω mesons for different input values of ρ_{00} and $\sigma_L = \sigma_T = 26$ mb is shown in Fig. 9. The nuclear transparency for ρ mesons is similar to ω mesons and corresponds to curves with $\rho_{00} = 0$, because ρ mesons are produced transversely polarized.

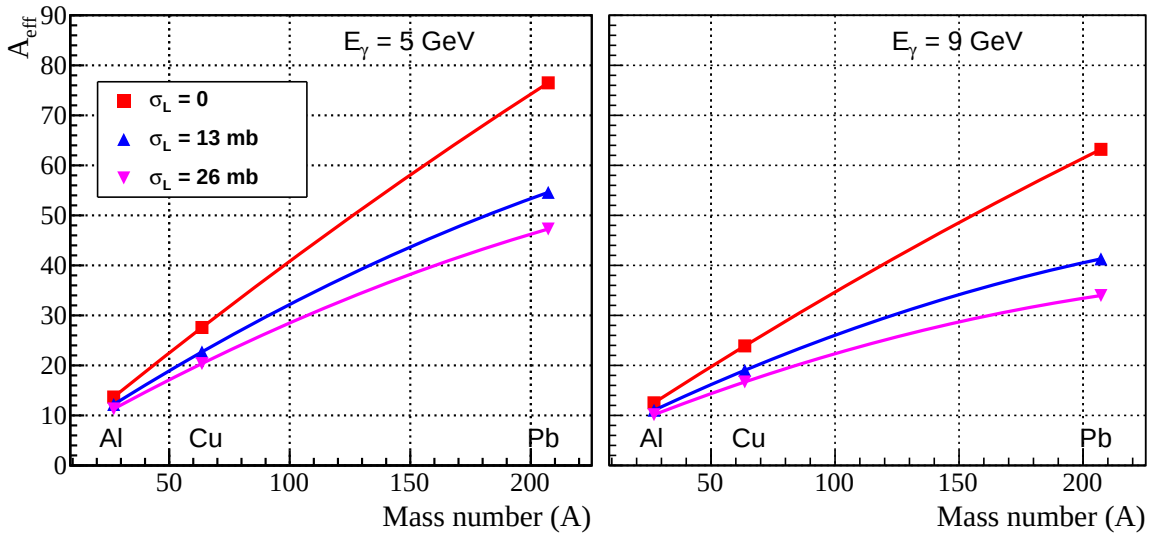

FIG. 6: A-dependence of the nuclear transparency A_{eff} for two beam energies: 5 GeV (left) and 9 GeV (right). The nuclear transparency is computed for different values of σ_L.

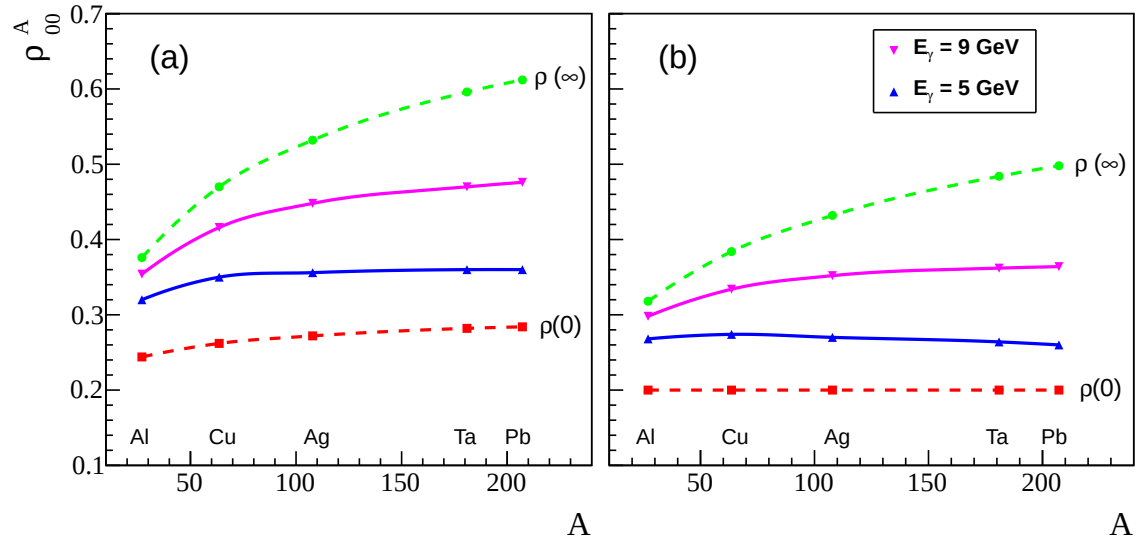

FIG. 7: A-dependence of the spin density matrix element ρ^A_{00} for (a) σ_L=13 mb and (b) σ_L=26 mb. ρ^A_{00} is shown for different photon energies. $\rho(\infty)$ and $\rho(0)$ correspond to infinite energy and energy-independent ρ^A_{00}, respectively.

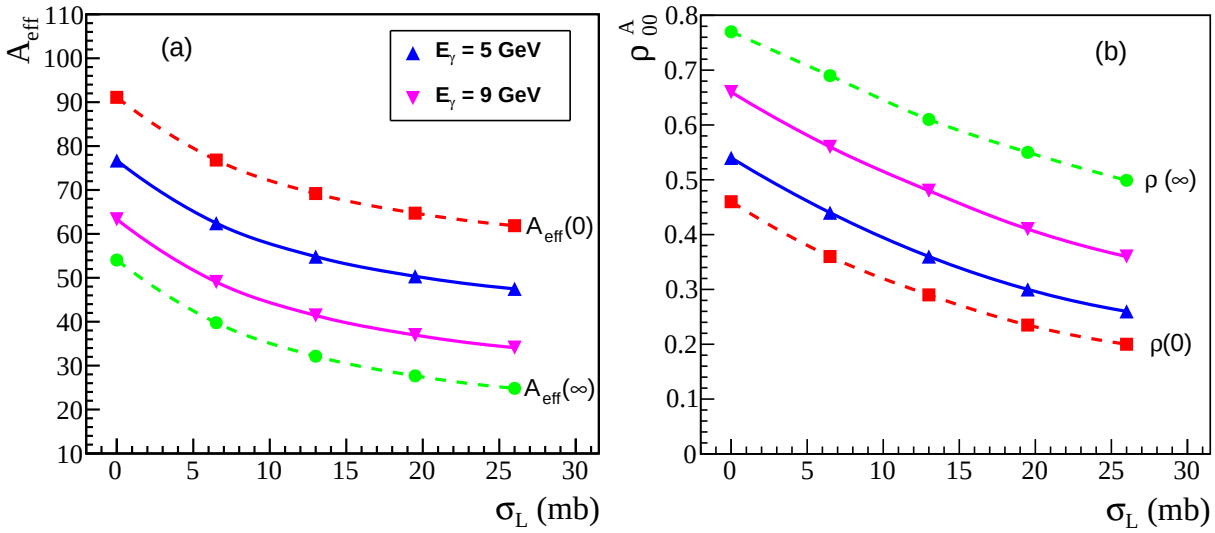

FIG. 8: (a) The nuclear transparency A_{eff} and (b) the spin density matrix element ρ^A_{00} as a function of σ_L for lead nucleus. The transverse ω-nucleon cross section σ_T and the spin density matrix element ρ_{00} are taken to be 26 mb and 0.2, respectively.

VI. RECONSTRUCTION OF VECTOR MESONS IN GLUEX

A. Reconstruction of ω mesons

We studied reconstruction efficiencies of ρ, ω, and ϕ mesons in the beam energy range between 6 GeV and 12 GeV using a detailed GlueX detector simulation. Mesons were generated in the $\gamma p \to Vp$ reaction using the Pythia event generator, which was adopted to account for the Fermi motion of nucleons. Generated events were passed through the GlueX Geant simulation and were reconstructed using the official GlueX reconstruction package.

The distribution of the invariant momentum transfer t for ω mesons generated by Pythia is presented in Fig. 10. The slope of the distribution is similar to SLAC measurements [2] ($t_0 = -7.5 \pm 0.8$ GeV^{-2} at the beam energy of 9 GeV). The typical GlueX reconstruction resolution for t for $\omega \to \pi^0\gamma$ decays in the range $t > 0.1$ GeV^2 is 0.016 GeV^2. Invariant mass distributions $m_{\gamma\gamma}$ and $m_{3\gamma}$ are presented on the bottom plots of Fig. 10. The invariant mass resolutions for reconstructed π^0 and ω mesons constitute about 7.7 MeV and 33 MeV, respectively. The missing-mass resolution is 190 MeV. The polar angle resolution of reconstructed $\omega \to \pi^0\gamma$ and $\omega \to \pi^+\pi^-\pi^0$ decays is about 0.1°. The angular acceptance of $\omega \to \pi^0\gamma$ decays in the helicity

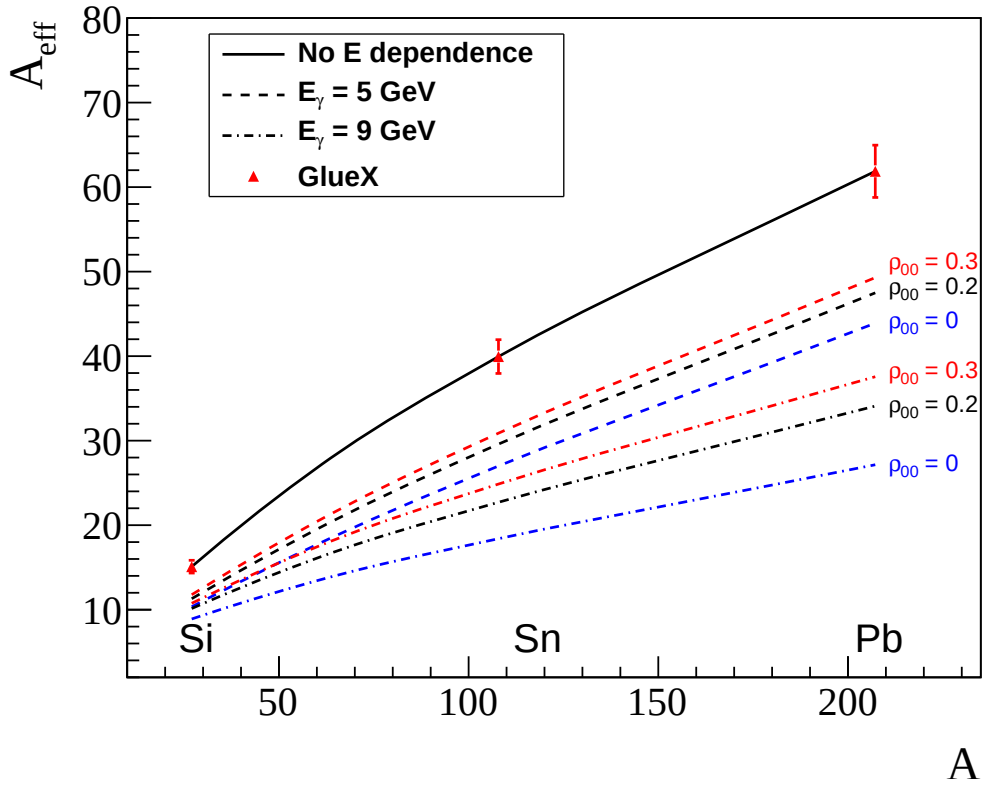

FIG. 9: Predicted energy dependence of the nuclear transparency for ω mesons for different input values of ρ_{00} and $\sigma_L = \sigma_T = 26$ mb. Similar dependence is expected for ρ mesons, assuming $\rho_{00} = 0$.

frame is shown in Fig. 11, where θ_H is the angle between the direction of the decay photon in the omega rest frame and the direction of omega meson in the c.m. system. The acceptance is uniform over the large range of cos $\theta_{\rm H}$, which is important for the measurement of the spin density matrix element ρ_{00} . The angular resolution $\Delta(\cos\theta_{\rm H})$ is $2.5 \cdot 10^{-2}$.

B. Reconstruction of ρ and ϕ mesons

We reconstruct ρ and ϕ mesons using $\rho \to \pi^+\pi^-$ and $\rho \to K^+K^-$ decay modes. The invariant mass distribution of ρ and ϕ candidates is presented in Fig. 12. Efficiencies to reconstruct ω, ρ, and ϕ mesons with the invariant momentum transfer 0.1 GeV$^2 < t <$ 0.5 GeV^2 and typical resolutions are listed in Table I. The relative dependence of the reconstructed efficiency on the beam energy is found to be relatively small, on the level of 15%.

VII. PRODUCTION OF VECTOR MESONS ON TARGET WALLS, GLUEX DATA

We studied capabilities to reconstruct ω mesons produced on nuclear targets by using the GlueX data with an empty target acquired in Spring 2017. In these data ω mesons can be produced on the target walls and the air downstream the target. The walls and the window are made from Kapton with the total thickness of about 280 μm, which corresponds to about $2 \cdot 10^{21}$ atoms/cm^2 (assuming that Kapton consists mostly of Carbon). The target cell contains some cold H_2 gas remaining after the liquid hydrogen was drained from the cell. The density of the H_2 gas is estimated to be about $1.8 \cdot 10^{-3}$ g/cm^3, which can be compared with the air density of $1.2 \cdot 10^{-3}$ g/cm^3. The total number of hydrogen atoms in the cell corresponds to

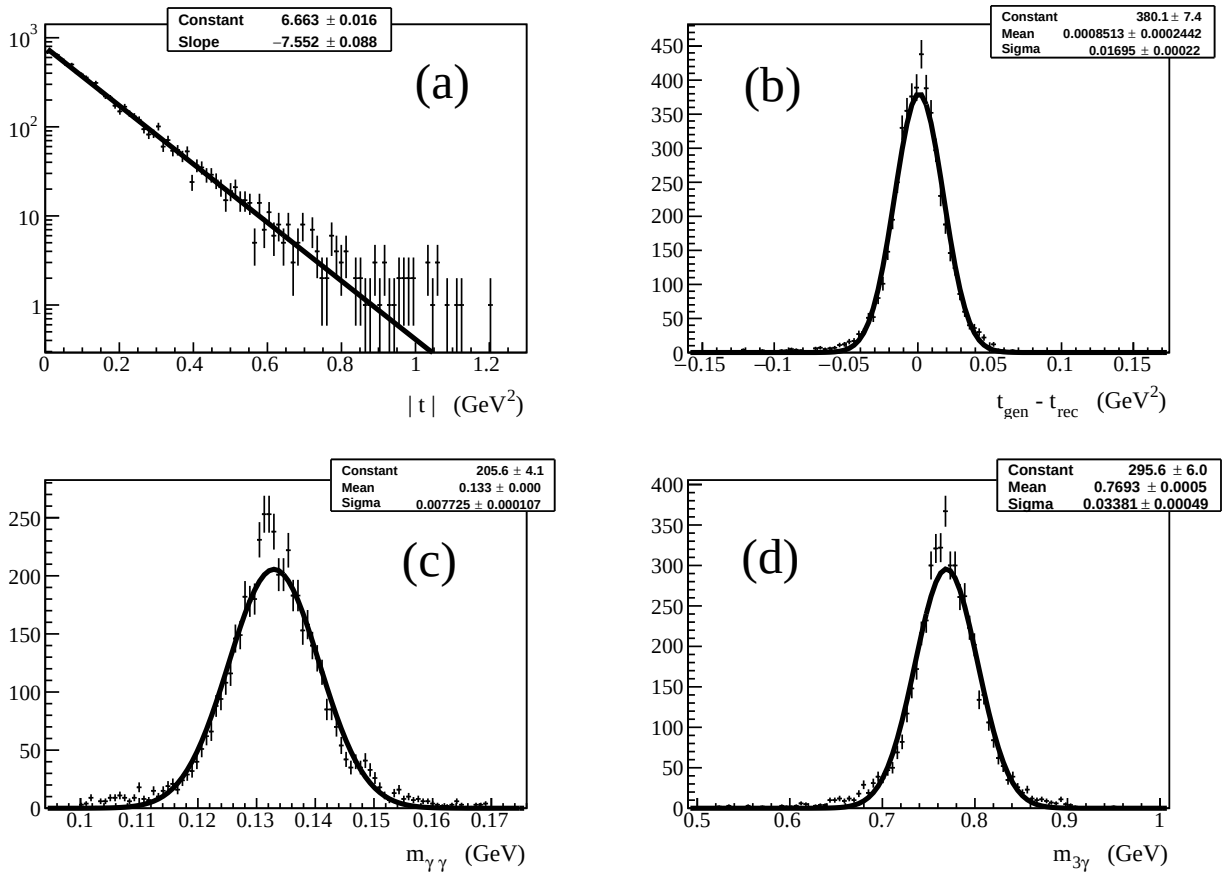

FIG. 10: Monte Carlo simulation for the reaction $\gamma p \to \omega p$, $\omega \to \pi^0\gamma$ (a) Distribution of the invariant transfer momentum generated by Pythia (b) Resolution of the transfer momentum, $t_{\rm gen} - t_{\rm rec}$ for $t > 0.1$ GeV^2 (c) Invariant mass $M_{\gamma\gamma}$ of reconstructed π^0 candidates (d) Invariant mass $M_{3\gamma}$.

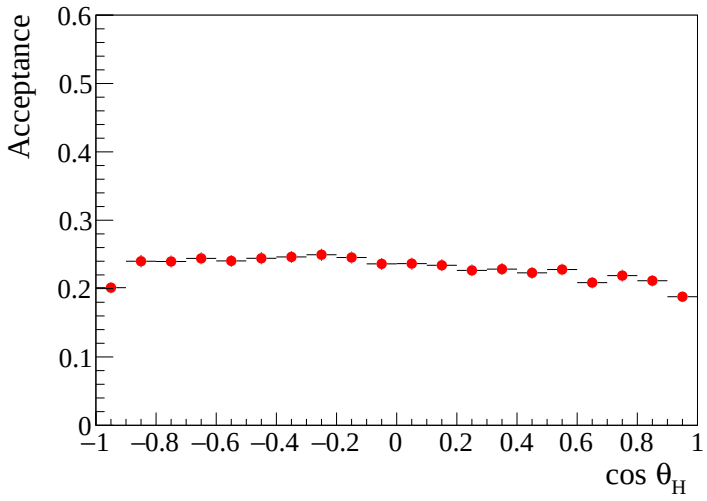

FIG. 11: Angular acceptance for $\omega \to \pi^0\gamma$ decays in the helicity frame.

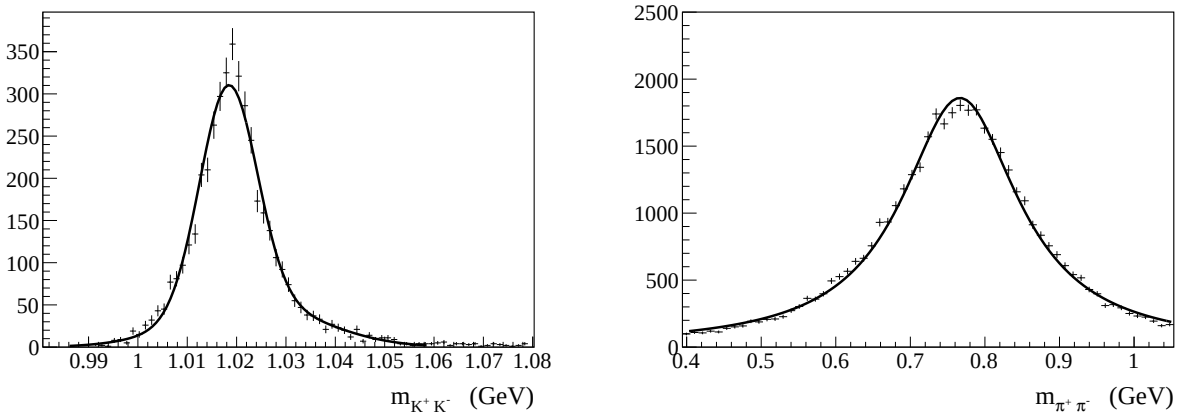

FIG. 12: Invariant mass distributions $M_{K^+K^-}$ (left) and $M_{\pi^+\pi^-}$ (right) of reconstructed ϕ and ρ candidates.

about $3.3 \cdot 10^{22}$ atoms/cm^2.

We select $\omega \to \pi^+\pi^-\pi^0$ candidates produced on the target walls or air by reconstructing the $\pi^\pm$ vertex. Z-coordinate of reconstructed vertices is presented in Fig. 13. Red arrows on this plot around the walls and air, denote Z-coordinates of vertices of ω candidates accepted for the analysis. We consider events with only two oppositely charged pion track candidates, a proton track consistent with the dE/dx of a proton hypothesis in the drift chambers, and a π^0 candidate. Events with extraneous reconstructed tracks or clusters in the calorimeters

	Final state			
	$\omega \to \pi^0\gamma$	$\omega \to \pi^+\pi^-\pi^0$	$\rho \to \pi^+\pi^-$	$\phi \to K^+K^-$
Branching Fraction (%)	8.28	89.2	1	48.9
Efficiency (%)	23.9	12.5	20.6	13.3
$\sigma(M_{\gamma\gamma})$ (MeV)	7.7	7.8		
$\sigma(M_{\omega})$ (MeV)	33	30		
$\sigma(M_{K^+K^-})$ (MeV)				7.1
σ(t) (GeV^2)	0.017	0.02	0.02	0.02
$\sigma(M_{mis})$ (MeV)	180	195	200	200

TABLE I: Reconstruction efficiencies and typical resolutions of ω, ρ, and ϕ mesons.

are rejected. The energy of reconstructed ω mesons is required to be larger than 6 GeV. The invariant mass distribution $M_{\pi^+\pi^-\pi^0}$ is presented in Fig. 14 for two types of events: (1) proton is reconstructed in the event (right plot) and (2) no proton candidate is found (left plot). A relatively small background is observed for $\omega \to \pi^+\pi^-\pi^0$ decays for events with and without a reconstructed proton.

For reconstruction of $\omega \to \pi^0\gamma$ decays we don't apply any constraints on the production vertex as there are no charged tracks in the final state except for some events with a recoil proton originating in the incoherent production on nuclei or in the $\gamma p \to \omega p$ reaction on the residual hydrogen gas in the target cell. The contribution to the production of ω mesons from the hydrogen gas is estimated to be smaller than that from nuclear photoproduction on the target walls and air. The invariant mass distribution $M_{3\gamma}$ is presented in Fig. 15. The ω peak on the mass distribution for events with no reconstructed proton (no vertex) is broad and shifted towards small masses. This can be accounted by the fact that ω mesons are produced on the air outside the target, at larger z, while in the reconstruction photons are assumed to originate from the center of the target, if vertex is not found. Under this assumption, the reconstruction angles between product decays are smaller than the real ones, resulting in the mass shift of π^0 and ω mesons. In the proposed experiment with a nuclear target, there will be no mass shift, as the position of the foil target is well defined. Background from ω production on air

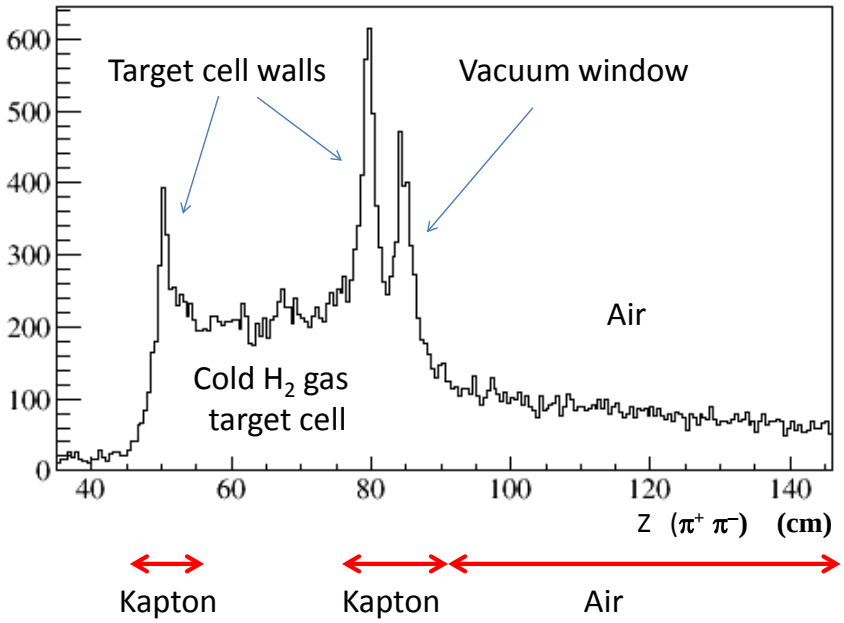

FIG. 13: Z-coordinate of reconstructed vertices of $\pi^{\pm}$ mesons originating from $\omega \to \pi^+\pi^-\pi^0$ candidates in runs with an empty target. The target cell is 30 cm long with the center positioned at Z = 65 cm.

and the target walls will be subtracted using runs with an empty target. As expected, there is no ω mass shift when a proton is reconstructed (see the right plot in Fig. 15). In this case the proton defines the production point for $\pi^0\gamma$. The signal to background ratio (S/B) for $\omega \to \pi^0\gamma$ is found to be relatively good, on the level of 2. In reality the S/B is expected to be better due to to the narrower mass distribution of reconstructed ω mesons on a thin target with a well-defined position. The invariant mass distribution $M(K^+K^-)$ for reconstructed ϕ meson candidates produced on the target walls is presented in Fig. 16. The background level for reconstructed ϕ meson candidates is found to be relatively small, $S/B \sim 3$.

VIII. RUN CONDITIONS

Photoproduction of vector mesons will be studied in the large beam energy range $E_\gamma > 6$ GeV using a photon beam produced by 11.6 GeV CEBAF electrons incident on an amorphous radiator. The energy of a beam photon is reconstructed by detecting bremsstrahlung electrons

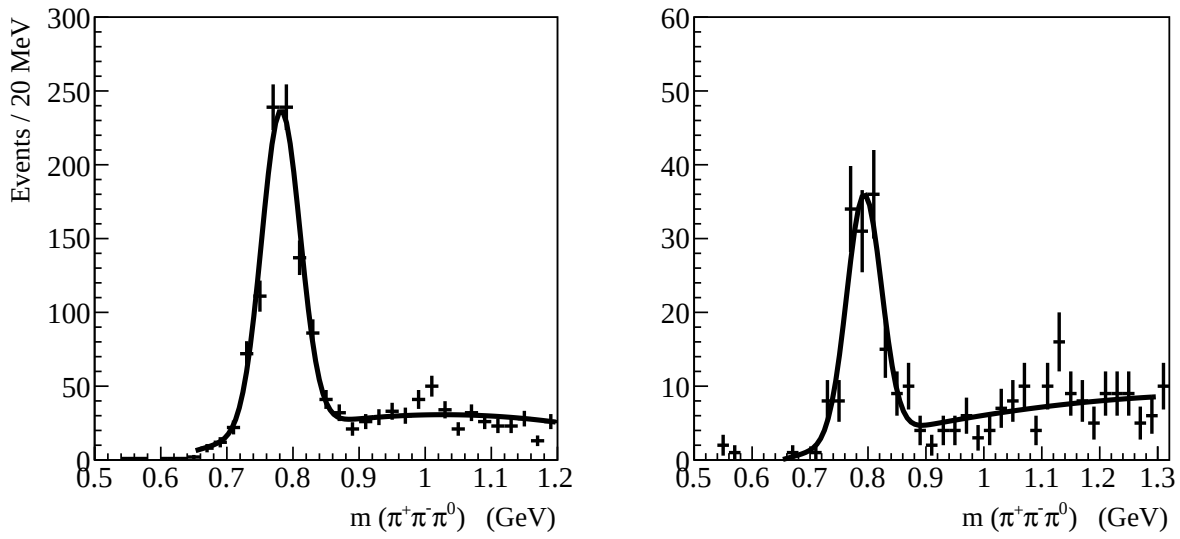

FIG. 14: Invariant mass distribution $M_{\pi^+\pi^-\pi^0}$ for events produced on target walls and air in runs with an empty target. The right plot corresponds to events with reconstructed proton. The left plot corresponds to events when no proton is found.

in the tagger hodoscope (TAGH) and microscope (TAGM) scintillator detectors. The tagging detectors provide a continuous energy coverage in the range between 7.8 GeV and 11.7 GeV and a typical electron detection efficiency of $90-95\%$. The TAGH counters are sampled below 7.8 GeV with an average sampling fraction of about 0.3. Reconstruction of the beam energy in the wide range is complicated due to the relatively large rate of accidental hits in the tagging detectors, i.e., hits originating from different events. In order to reduce the accidental rate, we are going to decrease the flux of uncollimated photons by a factor of 12 compared with the GlueX flux at high luminosity[4] and use larger collimator with a diameter of 5 mm. The fraction of events with multiple beam photons originating from the same beam bunch[5] in the energy between 6 GeV and 11.7 GeV is about 20%. The beamline conditions of the proposed experiment are listed in Table II.

We propose to use four nuclear targets: C, Si, Sn, Pb, with a thickness of 7% radiation length (the GlueX LH_2 target thickness is $3.5\%X_0$). Data will be taken on each individual target;

[4] The flux of collimated photons in GlueX in the coherent peak region is 5×10^7 γ/sec.
[5] Time spacing between beam bunches is 4 ns.

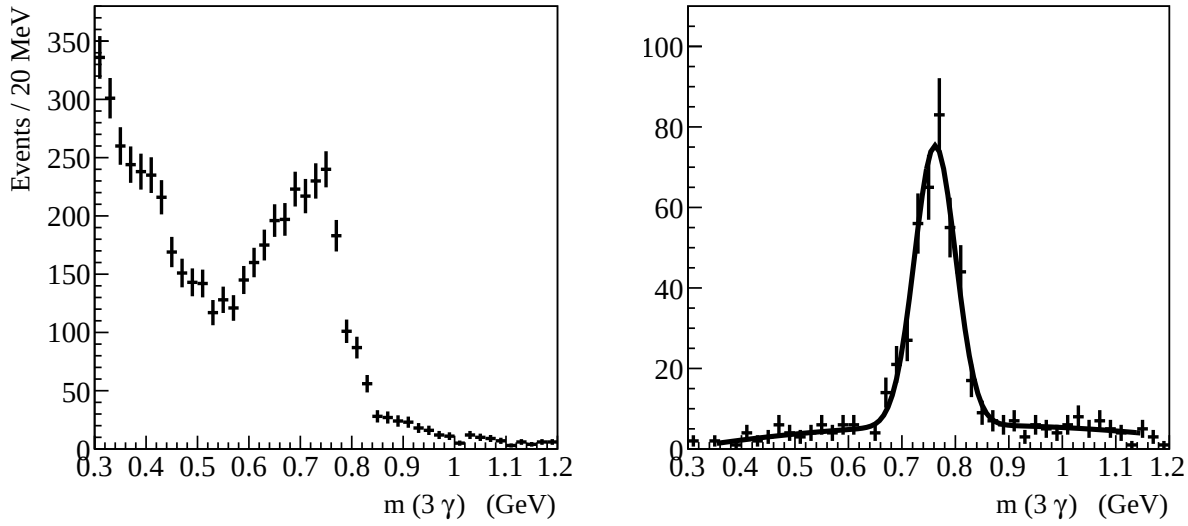

FIG. 15: Invariant mass distribution $M_{3\gamma}$ reconstructed in runs with an empty target. The right plot corresponds to events with reconstructed proton. The left plot corresponds to events when no proton is found.

multiple targets cannot be used in parallel due to the target misidentification in reconstruction of the multi-photon final state ($\pi^0\gamma$). Properties of nuclear targets are listed in Table III.

Reduction of the photon beam flux and using thin targets is also required by the electromagnetic and neutron backgrounds origination from nuclei. The neutron background is specifically critical for Silicon photomultipliers used in the barrel calorimeter and start counter. For the proposed run conditions, the electromagnetic background level (which is proportional to the photon flux and the target thickness in units of radiation lengths) is expected to be significantly smaller than for GlueX. The neutron background in the GlueX experiment was simulated using Geant provided by the RadCon group and Fluka for the LH_2 and liquid He targets [43]. The background induced by heavier nuclear targets can be scaled to He [44] and is not expected to exceed the GlueX level.

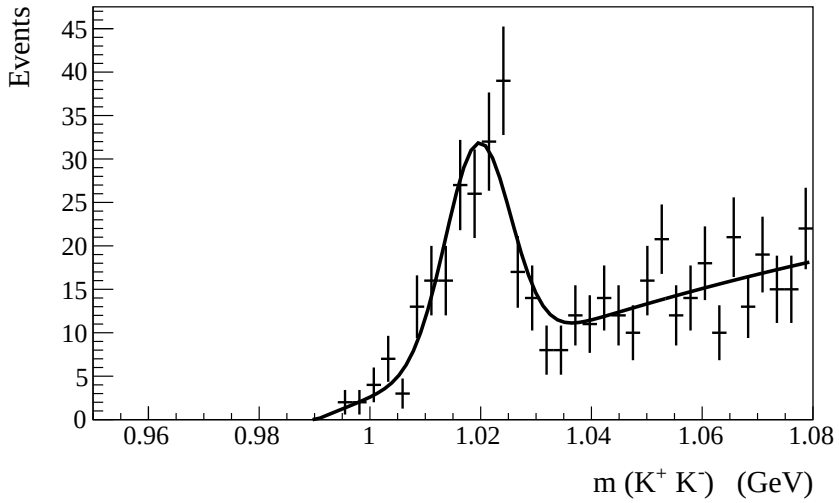

FIG. 16: Invariant mass distribution $M_{K^+K^-}$ for reconstructed ϕ meson candidates produced on the target walls.

Conditions	GlueX	Proposed Exp
Collimator (mm)	3.4	5
Radiator thickness (X_0)	$2 \cdot 10^{-4}$ (Diamond)	10^{-4} (Aluminum)
Beam current (μA)	1.1	0.18
Photon beam energy range of interest (GeV)	8.4 - 9.1	6 - 11.7
Rate of uncollimated photons (Hz)	$1.2 \cdot 10^8$	$5.3 \cdot 10^7$
Photon rate on target (Hz)	$5 \cdot 10^7$	$1.5 \cdot 10^7$

TABLE II: Beamline conditions of the proposed experiment compared with GlueX.

IX. PRODUCTION RATES AND BEAM TIME REQUEST

A. Production Rates

The number of reconstructed vector mesons produced in the incoherent process on different targets is given by the following expression:

	LH_2 (GlueX)	C	Si	Sn	Pb
A	1	12	28	119	207
Target thickness (X_0)	3.4%	7 %			
Relative EM background	1	0.3			
Number of atoms (N/cm^2)	$1.28 \cdot 10^{24}$	$1.5 \cdot 10^{23}$	$3.3 \cdot 10^{22}$	$3.1 \cdot 10^{21}$	$1.3 \cdot 10^{21}$
$N^{Target} \cdot A/N^{LH_2}$	1	1.4	0.7	0.3	0.2

TABLE III: Properties of nuclear targets proposed for the experiment.

$$N_{\rm rec} = N(A) \cdot N(\gamma) \cdot \sigma_{incoh} \cdot Br \cdot \epsilon, \tag{4}$$

where $N(A)$ is the number of atoms in the nuclear target, $N(\gamma)$ is the number of beam photons incident on the target, σ_{incoh} is the cross section of the incoherent photoproduction of mesons, Br is the branching ratio of the meson decay, and ϵ is the meson reconstruction efficiency.

We used the realistic photon beam flux and efficiencies in the tagging detectors simulated according to the run conditions described in Section 8. Cross sections of the incoherent photoproduction, σ_{incoh}, of ω, ρ, and ϕ mesons are listed in Table IV. The cross sections are shown for two beam energies, 6 GeV and 9 GeV. The reconstruction efficiencies are described in Section 7. The number of reconstructed mesons produced in the incoherent process on a C, Si, Sn, and Pb targets during one day of data taking is listed in Table V. We break down production rates into two beam energy ranges: [6 - 9] GeV and [9 - 12] GeV. The reconstructed mesons are required to have the momentum transfer in the range between [0.1 - 0.5] GeV^2. As an example, the number of reconstructed $\omega \to \pi^0\gamma$ decays produced on a Carbon target as a function of the beam energy is presented in Fig. 17.

B. Beam Time Request

We propose to measure nuclear transparencies for ω, ρ, and ϕ mesons for each nuclear target and two beam energy ranges, [6 - 9] GeV and [9 - 12] GeV, with the statistical error better than 2%. This will require to take data for 23 days on four nuclear targets. The profile of

Target	ω		ρ		ϕ	
	6 GeV	9 GeV	6 GeV	9 GeV	6 GeV	9 GeV
C	17	12	82	68	3.9	4.4
Si	30	20	137	107	7.3	8.2
Sn	75	45	341	220	21	22
Pb	119	67	546	325	36	34

TABLE IV: Cross sections of the incoherent photoproduction of ω, ρ, and ϕ mesons on different nuclear targets in units of μb.

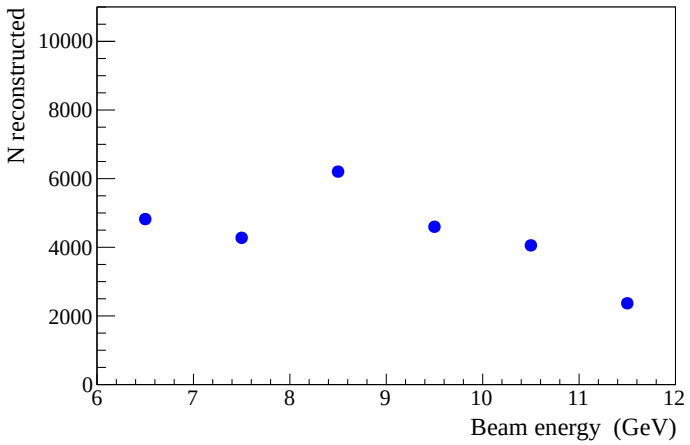

FIG. 17: The number of reconstructed $\omega \to \pi^0\gamma$ candidates produced in the incoherent process on a carbon target with the momentum transfer t between 0.1 GeV^2 and 0.5 GeV^2 as a function of the beam energy. The yield is normalized to 1 day of taking data.

.

the requested beam time is shown in Table VI. The number of reconstructed mesons produced in the incoherent process in the momentum transfer range between 0.1 GeV^2 and 0.5 GeV^2 is listed in Table VII.

In addition, we also require to take data for 3 days with an empty target. The data will be used to reduce uncertainties on the background subtraction of the non-target induced interaction. Two more days is need to perform the detector checkout with the beam and to calibrate

	$N_{\rm rec}$ per day ($\times 10^3$)							
	$\omega \to \pi^0\gamma$		$\omega \to \pi^+\pi^-\pi^0$		$\rho \to \pi^+\pi^-$		$\phi \to K^+K^-$	
Range (GeV)	6 - 9	9 - 12	6 - 9	9 - 12	6 - 9	9 - 12	6 - 9	9 - 12
C	19.3	13.4	112.9	78.5	1077.8	90.3	19.3	21.7
Si	7.1	4.7	41.4	27.7	38.1	30.0	7.9	8.6
Sn	1.6	0.9	9.5	5.6	82.8	52.9	2.1	2.1
Pb	1.0	0.6	6.0	3.3	52.3	30.1	1.4	1.3

TABLE V: The number of reconstructed ω, ρ, and ϕ mesons produced in the incoherent process on different nuclei targets. The mesons are required to be reconstructed in the t range between [0.1 - 0.5] GeV^2. The yield is normalized to 1 beam day.

Activity	Time (days)
C target	3
Si target	4
Sn target	6
Pb target	10
Empty target	3
Calibration and TAC runs	2
Total	28

TABLE VI: Beam time request.

acceptance of the Pair Spectrometer with the Total Absorption Counter. The calibration is needed for the photon flux determination. In conclusion, we are requesting a total of 28 days of the beam time.

	$N_{\rm rec}$ ($\times 10^3$)							
	$\omega \to \pi^0\gamma$		$\omega \to \pi^+\pi^-\pi^0$		$\rho \to \pi^+\pi^-$		$\phi \to K^+K^-$	
Range (GeV)	6 - 9	9 - 12	6 - 9	9 - 12	6 - 9	9 - 12	6 - 9	9 - 12
C	52.7	40.2	338.7	235.5	3233	270.9	57.9	65.1
Si	28.4	18.8	165.6	110.8	152.4	120.0	31.6	34.4
Sn	9.6	5.4	57.0	33.6	496.8	317.4	12.6	12.6
Pb	10.0	6.0	60.0	33	523	301	14	13

TABLE VII: Expected number of reconstructed ω, ρ, and ϕ mesons during 23 days of taking data with four nuclear targets.

X. UNCERTAINTIES AND SENSITIVITY

The data analysis will be organized into several steps:

1. We will measure total photoproduction cross sections of ω, ρ, and ϕ mesons on four nuclear targets in the beam energy range between 6 GeV and 12 GeV and compute the nuclear transparency $A_{eff} = \sigma_A/\sigma_N$, which will be used to
   - Study the dependency of the nuclear transparency on the beam energy
   - Extract the cross section of the longitudinally polarized ω mesons with nucleons $\sigma_L(\omega N)$ according to the predicted dependence of A_{eff} on σ_L given by Eq. 2.
2. We will measure the spin density matrix element ρ^A_{00} on nuclear targets and extract $\sigma_L(\omega N)$ using the predicted dependence of ρ^A_{00} on σ_L given by Eq. 3.

Reconstruction of ω mesons will be performed using two decay modes, $\omega \to \pi^0\gamma$ and $\omega \to \pi^+\pi^-\pi^0$. In this section we discuss uncertainties on the measurements of A_{eff} and ρ^A_{00} and projected errors on the extracted value of $\sigma_L(\omega N)$.

A. Measurement of $A_{\rm eff}$ and extraction of $\sigma_L(\omega N)$

1. Measurement of $A_{\rm eff}$

The statistical error on the measurement of photoproduction cross sections on each target is estimated to be less than 2%. According to Table 7, the smallest data sample of $\omega \to \pi^0\gamma$ decays will be acquired on a lead target in the energy range between 9 GeV and 12 GeV, and will contain about 6000 reconstructed events. In Section 7 we described the reconstruction of ω mesons produced on the target walls using GlueX data with an empty target. Based on these studies we conservatively assume that the background level should not exceed the signal. Statistical errors on measured cross sections for this decay channel are estimated to be 1.4% and 1.8% for two beam energy ranges [6 - 9] GeV and [9 - 12] GeV, respectively. We expect that uncertainties on the measurement of the nuclear transparency will be dominated by systematic errors.

We note that some of the systematic uncertainties on A_{eff} related to reconstruction efficiencies will be partially canceled out since the nuclear transparency represents the ratio of two cross sections σ_A/σ_N. The cross section σ_A will be measured in the proposed experiment, while the meson production cross section on the nucleon σ_N will be independently obtained using a high-statistic data sample acquired by the GlueX experiment. In the analysis of experimental data acquired on different nuclear target, ω mesons will be reconstructed using the same event selection criteria. The uncertainty on the target thickness (number of atoms) is 1.2%. The photon flux will be measured using the pair spectrometer, which can provide a precision of 1.5% [41]. The major contribution to the systematic error is expected to originate from the signal yield determination (background subtraction). We estimate uncertainties on the signal yield due to the background shape using a Monte Carlo simulation. MC samples were generated according to different background shapes and assuming the signal to background ration to be equal to one in the signal region. The background shape was obtained from the fit to the generated distribution. We varied the fit parameters by one standard deviation and observed changes in the signal yield. We also varied the width of the invariant mass distribution of the meson, which was a free parameter in the fit. Changes of the signal yield were on the level of 3%. Systematic uncertainties on A_{eff} are listed in Table VIII. Also the theoretical prediction of the nuclear transparency A_{eff} with the superimposed projected errors is presented on the left

plot of Fig. 20. As a result, the overall estimated systematic uncertainty on the measurement of A_{eff} is 5.4%.

Source	Uncertainty (%)
Target thickness	1.2
Photon flux determination	1.5
Signal yield (bg subtraction)	5.0
Uncertainty on A_{eff}	5.4

TABLE VIII: Systematic uncertainties on the measurement of the nuclear transparency $A_{\rm eff}$.

2. Extraction of $\sigma_L(\omega N)$ from $A_{\rm eff}$

The cross section $\sigma_L(\omega N)$ is extracted from the measured A_{eff} using theoretical predictions described in Section 5. We obtain σ_L from the fit of the measured A-dependency of the nuclear transparency to the theoretically predicted function given by Eq. 2. Nuclear transparency as a function of the mass number A is presented on the left plot of Fig. 20. Two curves on this plot correspond to theoretical predictions computed for two values of $\sigma_L = 13$ mb and $\sigma_L = 26$ mb. Theoretical predictions depend on the fraction of longitudinally polarized mesons through the parameter ρ_{00} in Eq. 2. The spin density matrix element ρ_{00} will be measured by the GlueX experiment in the exclusive photoproduction of ω mesons on a proton with the precision of $\delta(\rho_{00}) \sim 0.02$, see Appendix A. Preliminary GlueX results indicate that the value of ρ_{00} is close to the previous SLAC measurement of $\rho_{00} \sim 0.2$ even at large beam energies around 9 GeV. The impact of ρ_{00} to the fit function is discussed in Appendix B. We vary the value of ρ_{00} in the fit function by ± 0.02, and the maximum observed shift of σ_L obtained from the fit was assigned as a systematic uncertainty on σ_L due to ρ_{00}.

Uncertainties on the extracted value of σ_L are evaluated using Monte Carlo simulation. We generate a set of A_{eff} corresponding to different targets. Values of A_{eff} are distributed according to the statistical and systematic errors around central values which are set according to the theoretical prediction. The MC sample is generated for the specific value of σ_L. We subsequently fit the generated nuclear transparency distribution to the theoretical function for

Fraction of polarized	Uncertainty on σ_L (mb)	
ω mesons	6 - 9 GeV	9 - 12 GeV
$\rho_{00} = 0.2$	0.9 (stat) 3.4 (syst)	0.9 (stat) 3.1 (syst)
$\rho_{00} = 0.14$	1.1 (stat) 4.6 (syst)	1.1 (stat) 4.2 (syst)

TABLE IX: Uncertainties on σ_L (for σ_L = 16 mb) extracted from the measurement of A_{eff} for two fractions of linearly polarized ω mesons, $\rho_{00} = 0.2$ and $\rho_{00} = 0.14$.

the parameter σ_L. Uncertainties on σ_L (for σ_L equals to 16 mb) obtained from the fit are listed in Table IX. In this table, we break down contributions from the statistical and systematic errors on A_{eff}. Uncertainties on σ_L are obtained for two input values of $\rho_{00} = 0.2$ and $\rho_{00} = 0.14$. As expected, the precision on the determination of σ_L depends on the fraction of longitudinally polarized ω mesons; better precision is achieved for larger values of ρ_{00}. The systematic error on σ_L consists of uncertainties from the measurement of A_{eff} and theoretical model dependence on ρ_{00}; these two contributions are added in quadrature. As an example, uncertainties on σ_L due to ρ_{00} (for $\rho_{00} = 0.14$) for two beam energy ranges 6–9 GeV and 9–12 GeV are 2.1 mb and 2.5 mb, respectively. This can be compared with the total systematic errors of 4.6 mb and 4.2 mb.

B. Measurement of ρ_{00}^A and extraction of $\sigma_L(\omega N)$

1. *Measurement of* ρ_{00}^A

We estimated statistical errors on the measurement of ρ_{00}^A using Monte Carlo simulation. MC samples were generated according to different input values of ρ_{00}. We take into account the realistic angular acceptance of the detector and signal to background ratios. The value of ρ_{00}^A is obtained from the fit to the decay angular distribution of ω mesons in the helicity frame. The angular distribution for $\omega \to \pi^+\pi^-\pi^0$ decays can be written as

$$W(\cos\theta_H) \sim \frac{1}{2} \cdot (1 - \rho_{00}) \cdot \sin^2\theta_H + \rho_{00} \cdot \cos^2\theta_H, \tag{5}$$

where θ_H is the angle between the normal of the ω decay plane in the ω rest frame with respect to the ω meson direction in the c.m. system. The polar angular distribution generated

according to the input values of $\rho_{00} = 0.2$ and the signal to background ratio equals to one is presented in Fig. 18. Statistical errors on ρ_{00}^A for the smallest data sample of $\omega \to \pi^0\gamma$ decays acquired by the proposed experiment (see Table VII) are $\sigma(\rho_{00}^A) = 0.011$ and $\sigma(\rho_{00}^A) = 0.014$ for two beam energy ranges [6 - 9] GeV and [9 - 12] GeV, respectively. The statistical error does not depend on the input value of ρ_{00}.

Measurement of the spin density matrix elements does not require information about normalization. Systematic uncertainties on the measurement of ρ_{00}^A will be dominated by the signal yield extraction (background subtraction) and determination of the angular acceptance. In order to study the dependence of ρ_{00}^A on the signal yield we generated MC samples according to different values of ρ_{00}^A. We varied the yield of ω mesons by $\pm 5\%$ and observed the change of the fit parameter ρ_{00}^A. The maximum deviation of 0.008 was assigned as a systematic error on ρ_{00}^A due to uncertainties in the signal yield. The angular acceptance for ω mesons is uniform over almost the whole range of $\cos\theta_H$, resulting in the small angular-dependent acceptance corrections. The acceptance for $\omega \to \pi^0\gamma$ decays is presented in Fig. 11. Based on the quality of the GlueX experimental data, we estimated the systematic uncertainty on ρ_{00}^A due to the acceptance corrections to be 0.019, which is typical for the high-statistic measurement of the spin density matrix element ρ_{00} [42]. The total systematic error on the measurement of ρ_{00}^A is 0.02. Systematic uncertainties on the measurement of the spin density matrix element ρ_{00}^A are listed in Table XI. Theoretical predictions of the A-dependence of the spin density matrix element ρ_{00}^A computed for two values of $\sigma_L = 13$ mb and $\sigma_L = 26$ mb are presented on the right plot of Fig. 20. Projected errors on ρ_{00}^A from the proposed experiment are superimposed on this plot.

Fraction of polarized	Uncertainty on σ_L (mb)	
ω mesons	6 - 9 GeV	9 - 12 GeV
$\rho_{00} = 0.2$	1.0 (stat) 3.6 (syst)	1.1 (stat) 3.5 (syst)
$\rho_{00} = 0.14$	1.1 (stat) 4.7 (syst)	1.2 (stat) 4.6 (syst)

TABLE X: Uncertainties on σ_L (for $\sigma_L = 16$ mb) extracted from the measurement of ρ_{00}^A for two fractions of linearly polarized ω mesons, $\rho_{00} = 0.2$ and $\rho_{00} = 0.14$.

2. *Extraction of $\sigma_L(\omega N)$ from ρ^A_{00}*

The cross section $\sigma_L(\omega N)$ is extracted according to the predicted dependence of ρ^A_{00} on σ_L, described in Section 5. The value of σ_L is obtained from a fit of the measured A-dependency of the the spin density matrix element ρ^A_{00} to the function given by Eq. 3. The typical shape of the fit function is shown on the right plot of Fig. 20. We take into account uncertainties on the input parameter ρ_{00} in Eq. 3 and vary the value of ρ_{00} according to one standard deviation, $\delta(\rho_{00}) = \pm\ 0.02$. The observed shift of the fit parameter σ_L is attributed as the systematic uncertainty due to ρ_{00}.

Similar to the extraction of σ_L from A_{eff}, we evaluate uncertainties on σ_L using MC simulation. A set of ρ^A_{00} values is generated corresponding to different targets for the specific value of σ_L. The values of ρ^A_{00} are distributed according to the predicted statistical and systematic errors. The cross section σ_L is then retrieved from the fit to the generated distribution. Uncertainties on σ_L (for σ_L equals to 16 mb) obtained from the fit are listed in Table X. Errors on σ_L are estimated for two fractions of linearly polarized ω mesons, $\rho_{00} = 0.2$ and $\rho_{00} = 0.14$. The major contribution to the systematic error of σ_L comes from the uncertainty on the spin density matrix element ρ_{00}.

Source	Uncertainty (%)
Signal yield (bg subtraction)	0.008
Acceptance determination	0.019
Uncertainty on ρ^A_{00}	0.02

TABLE XI: Systematic uncertainties on the measurement of spin density matrix element ρ^A_{00}

C. Projected errors on $\sigma_L(\omega N)$

The cross section σ_L will be extracted from the nuclear transparency A_{eff} and spin-density matrix element ρ^A_{00} independently. We combine uncertainties on σ_L obtained from measurements of A_{eff} and ρ^A_{00} using two decay modes of ω mesons: $\omega \to \pi^0\gamma$ and $\omega \to \pi^+\pi^-\pi^0$. The projected errors on σ_L are listed in Table XII. We used a weighted average to combine independent statistical and uncorrelated part of systematic errors on σ_L. The correlated part of the

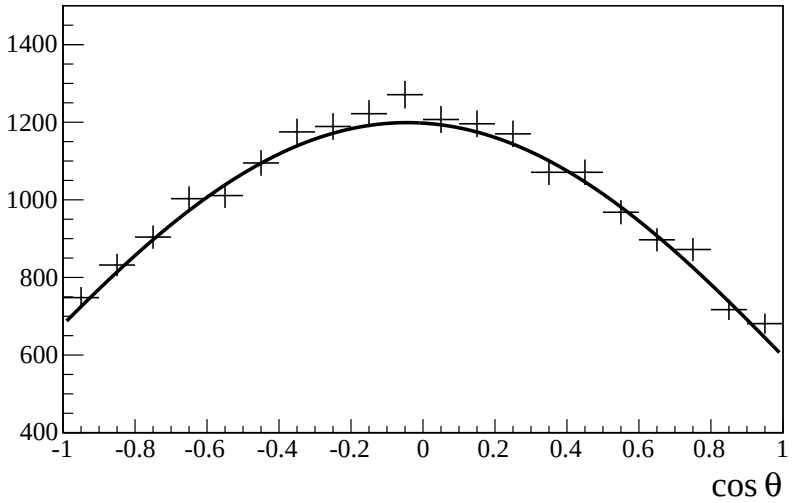

FIG. 18: Monte Carlo simulation of the polar angular distribution of $\omega \to \pi^+\pi^-\pi^0$ decays with the background in the helicity frame.

systematic error is associated with uncertainties on ρ_{00} and cannot be improved by performing multiple measurements. This error is added in quadrature with the statistical and uncorrelated systematic errors. As an example, the correlated error on σ_L extracted from the A_{eff} (for $\rho_{00} = 0.14$) is $\delta(\sigma_L) = 2.2$ mb and $\delta(\sigma_L) = 2.6$ mb for two beam energy ranges 6–9 GeV and 9–12 GeV.

Fraction of polarized ω mesons	Uncertainty on σ_L (mb)			
	A_{eff}		ρ_{00}^A	
	6 - 9 GeV	9 - 12 GeV	6 - 9 GeV	9 - 12 GeV
$\rho_{00} = 0.2$	2.7	2.6	3.4	3.3
$\rho_{00} = 0.14$	3.7	3.5	4.5	4.4

TABLE XII: Uncertainties on σ_L (for $\sigma_L = 16$ mb) extracted from the measurements of A_{eff} and ρ_{00}^A using $\omega \to \pi^0\gamma$ and $\omega \to \pi^+\pi^-\pi^0$ decay channels.

Cross sections σ_L and σ_T predicted by the two theoretical models described in Section 2.C are presented in Fig. 19. Projected errors on σ_L obtained from the measurement of A_{eff} are

superimposed on this plot. Independent extraction of σ_L from the nuclear transparency and spin density matrix elements will provide control of systematics.

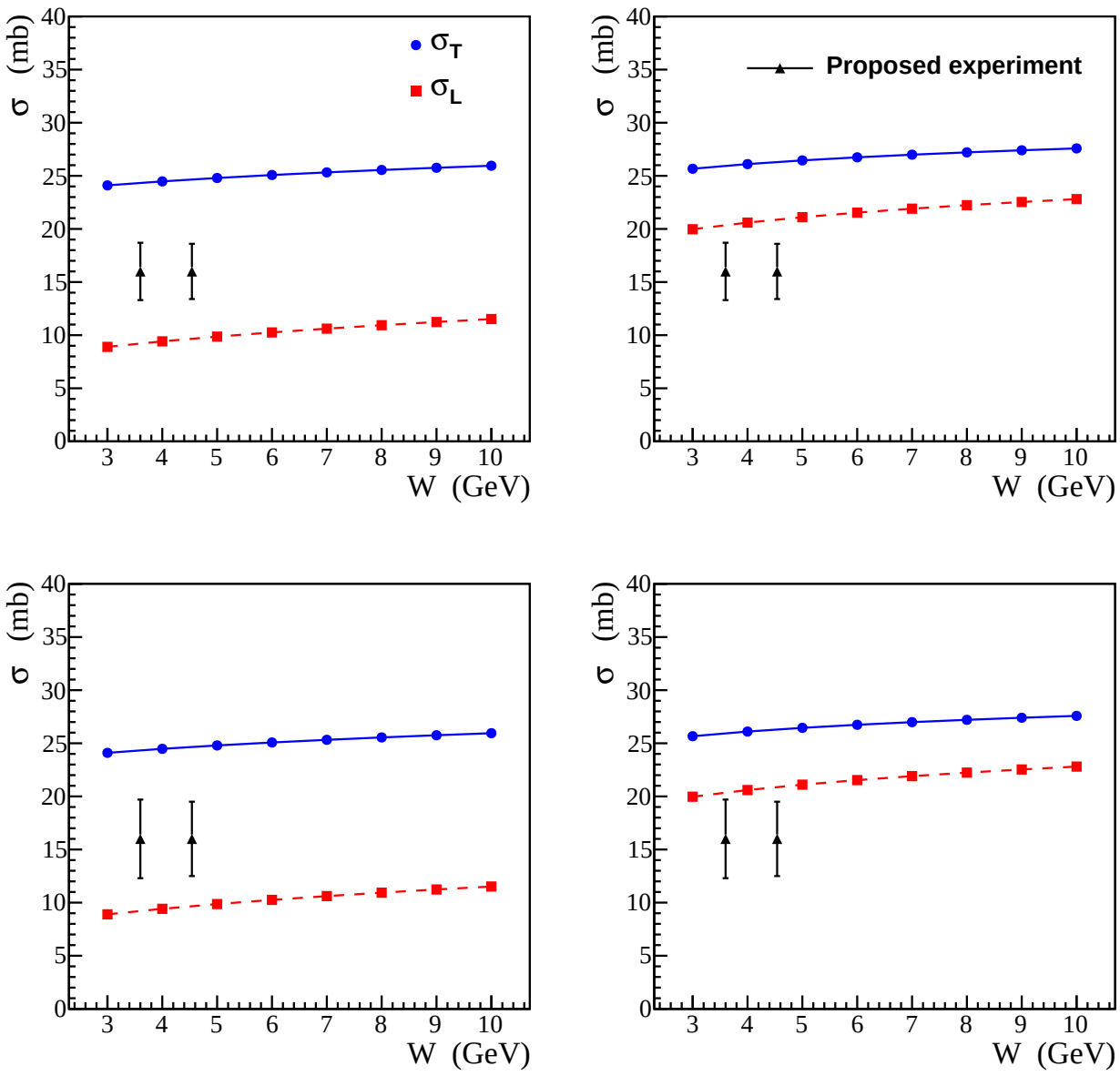

FIG. 19: Cross sections σ_L and σ_T predicted by the two theoretical models described in Section 2 are shown on the left and right plots. Projected errors on σ_L of the proposed experiment obtained from the measurement of A_{eff} using $\omega \to \pi^0\gamma$ and $\omega \to \pi^+\pi^-\pi^0$ decays (circles with error bars). σ_L was extracted using two input values of the spin-density matrix element $\rho_{00} = 0.2$ (top) and $\rho_{00} = 0.14$ (bottom).

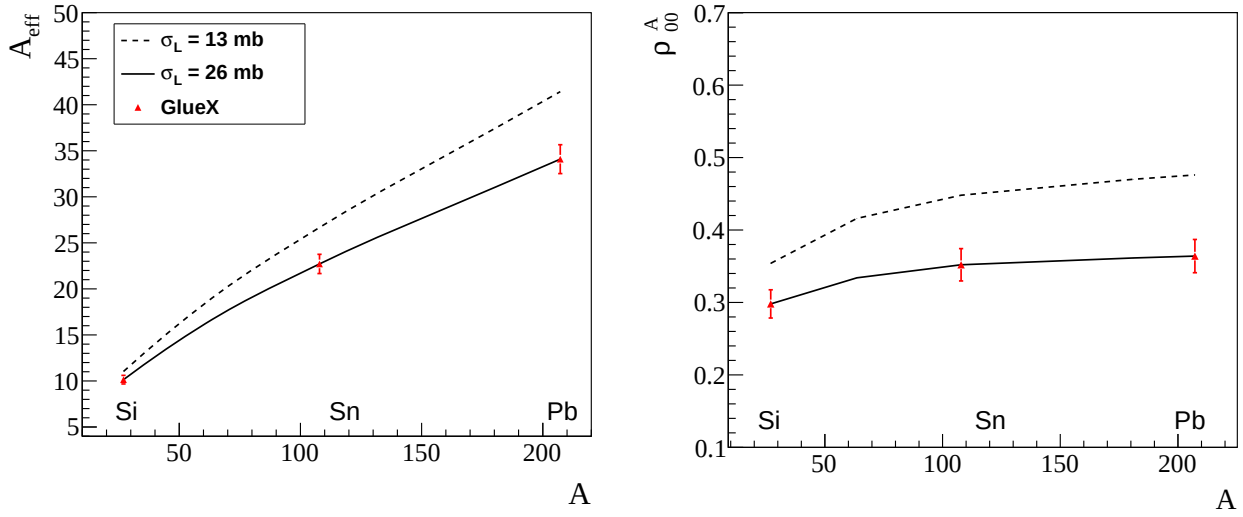

FIG. 20: A-dependence of the nuclear transparency A_{eff} (left) and the spin density matrix element ρ^A_{00} (right) for two values of σ_L and the beam energy of 9 GeV. The curves were computed for $\rho_{00} = 0.2$. Markers correspond to the projected errors of the proposed experiment.

XI. SUMMARY

We request 28 days of beam time to measure photoproduction cross sections of light vector mesons (ρ, ω, ϕ) on four nuclear targets (^{12}C, ^{28}Si, ^{120}Sn, and ^{208}Pb) using a tagged photon beam of 6–12 GeV. The nuclear transparency (A_{eff}) and the spin density matrix element (ρ^A_{00}) of these mesons will be extracted with the precision of $\sim 5\%$ and $\sim 10\%$, respectively. These measurements will impact several important issues:

1. Measurements of a beam energy dependence of the nuclear transparency over a wide energy range between 6 GeV and 12 GeV for three light mesons (ρ, ω, ϕ) will shed light on a long standing puzzle: a weak beam-energy dependence of the nuclear transparency observed in the previous experiments [7–9], that contradicts the theoretical predictions [5, 6]. These results will also provide a sensitive probe to the degree of photon shadowing in nuclear matter.

2. For the first time, the total cross section of longitudinally polarized ω mesons on a nucleon, $\sigma_L(\omega N)$, will be extracted from the two independent measurements of A_{eff} and ρ^A_{00} in the incoherent ω photoproduction. These two different methods will provide a cross check of systematic uncertainties. The knowledge of $\sigma_L(\omega N)$ is important for many theoretical models. It will also provide important information for understanding the color transparency in the electroproduction of vector mesons.

The data sample acquired in the proposed experiment will allow to study other physics topics, such as the absorption of different projections of the total orbital momentum of a tensor meson $f_2(1270)$[6]. Studies of the nuclear transparency in photoproduction of vector mesons can also be extended to the region of the larger transfer momenta $\mid t \mid > 1 - 2$ GeV^2, where the color transparency effects can be investigated.

We will perform the experiment with the GlueX detector at relatively low luminosity. No modifications of the GlueX detector except replacement of the LH_2 target with the nuclear targets are required.

[6] $f_2(1270)$ meson can be clearly reconstructed with the GlueX detector

APPENDIX A: MEASUREMENT OF THE SPIN-DENSITY MATRIX ELEMENT ρ_{00}

The fraction of longitudinally polarized ω mesons is given by the spin-density matrix element ρ_{00}, which can be obtained from the fit to the ω decay angular distribution in the helicity frame. ρ_{00} was originally measured in a bubble chamber experiment at SLAC in the $\gamma p \to \omega p$ reaction with small statistics. The experiment measured $\rho_{00} = 0.2 \pm 0.07$ at 9.3 GeV beam energy [2].

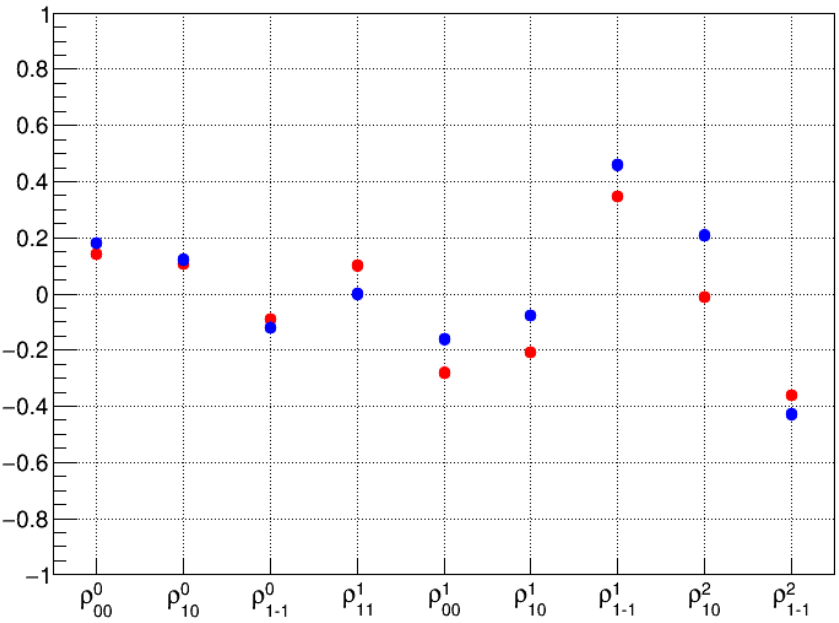

FIG. 21: Preliminary results from the ongoing analysis of $\omega \to \pi^0\gamma$ decays. Spin-density matrix elements measured using a beam of polarized photons in the energy range between 8.4 GeV and 9 GeV. Red and blue circles correspond to two orientations of the photon beam polarization. The plot is taken from [45].

ρ_{00} will be independently measured by the GlueX experiment in the $\gamma p \to \omega p$ reaction using a large data sample of reconstructed ω mesons in $\omega \to \pi^0\gamma$ and $\omega \to \pi^+\pi^-\pi^0$ decay modes. The first ongoing analysis of the GlueX data indicates that the value of ρ_{00} is larger than 0.1. Spin-density matrix elements obtained from runs with a polarized photon beam in the energy range between 8.4 GeV and 9.0 GeV are presented in Fig 21. Measurement of the spin density matrix elements does not require information about normalization, the systematic error will be dominated by the angular acceptance correction. The GlueX experiment is well suited for angular analyses of $\omega \to \pi^0\gamma$ and $\omega \to \pi^+\pi^-\pi^0$ decays because of a uniform angular acceptance.

Based on the quality of the GlueX experimental data, we estimate the dominant systematic error on the ρ_{00} determination to be better than 0.02 (which corresponds to the relative error of 10% for $\rho_{00} = 0.2$). Such precision has been achieved by other experiments, specifically by CLAS, who studied photoproduction of ω mesons at small energies [42].

APPENDIX B: SENSITIVITY OF A_{eff} AND ρ_{00}^{A} TO ρ_{00}

Theoretical dependence of the nuclear transparency A_{eff} and ρ_{00}^{A} on ρ_{00} is given by Eq. 2 and Eq 3 and is presented below.

- **Nuclear transparency** A_{eff}

$$A_{eff} \;=\; \rho_{00}N(0,\sigma_L) + (1-\rho_{00})N(k,\sigma_T) \tag{B1}$$

The relative deviation of A_{eff} due to the uncertainty of ρ_{00} can be written as

$$\frac{\delta(A_{eff})}{A_{eff}} \;=\; \frac{N(0,\sigma_L) - N(k,\sigma_T)}{\rho_{00}N(0,\sigma_L) + (1-\rho_{00})N(k,\sigma_T)}\delta(\rho_{00}) \tag{B2}$$

$\delta(A_{eff})/A_{eff}$ depends on the target material, beam energy, and values of σ_L and ρ_{00}. The maximum deviation of A_{eff} for $\delta(\rho_{00}) = \pm\, 0.02$ (and $\rho_{00} = 0.14$) is 3.2%.

- **The spin-density matrix element** ρ_{00}^{A}

$$\rho_{00}^{A} = \frac{N(0,\sigma_L)}{\rho_{00}N(0,\sigma_L) + (1-\rho_{00})N(k,\sigma_T)}\rho_{00} \tag{B3}$$

The deviation of $\delta(\rho_{00}^{A})$ is given by

$$\delta(\rho_{00}^{A}) = \frac{N(0,\sigma_L)N(k,\sigma_T)}{\rho_{00}N(0,\sigma_L) + (1-\rho_{00})N(k,\sigma_T))}\delta(\rho_{00}) \tag{B4}$$

The maximum deviation of $\delta(\rho_{00}^{A})$ for $\delta(\rho_{00}) = \pm\, 0.02$ (and $\rho_{00} = 0.14$) is 0.032.

[1] E. Chudakov, S. Gevorkyan, A. Somov, Phys. Rev. C93,015203 (2016).

[2] J. Ballam et al., Phys. Rev. D7,3150 (1973).

[3] D. Dutta, K. Hafidi, M. Strikman, Prog. Part. Nucl. Phys. 69, 1 (2013).

[4] A. Airapetian et al., Eur. Phys. J. C 64, 659 (2009).

[5] T. Bauer, R. Spital, D. Yennie, F. Pipkin, Rev.of Mod. Phys. 50, 261 (1978).

[6] K. Gottfried, D.Yennie, Phys. Rev. 182, 1595 (1969).

[7] G. McClellan et al., Phys. Rev. Lett. 23,554 (1969).

[8] A. M. Boyarski et al., Phys. Rev. Lett. 23, 1343 (1969).

[9] W. T. Meyer et al. Phys. Rev. Lett. 28,1344 (1972).

[10] P. Joos et al., Nucl. Phys. B113, 53 (1976).

[11] R. Dixon et al. Phys. Rev. Lett. 39,516 (1977).

[12] J. Sakurai, D. Schildknecht, Phys. Lett. 40B, 121 (1972).

[13] V. Franco, R. Glauber, Phys. Rev. Lett. 22, 370 (1969).

[14] L. Azhgirey et al., Phys. Part. Nucl.Lett. 5,728 (2008); 7,27 (2010).

[15] H. Seyfarth et al., Phys. Rev. Lett. 104, 222501 (2010).

[16] L. Gerland et al., Phys. Rev. Lett. 81, 762 (1998).

[17] I. P. Ivanov, N.N. Nikolaev, A.A. Savin, Physics of Particles and Nuclei 37,5 (2006).

[18] W. Jaus, Phys. Rev. D44, 2851 (1991).

[19] A. V. Arefyev et.al, Sov. J. Nucl. Phys. 19, 304 (1974); 27, 85 (1978).

[20] A. S. Pak, A. V. Tarasov, Yad. Phys. 22, 91 (1975).

[21] B. Chaudhary et al., Nucl. Phys. B67, 333 (1973).

[22] S. Gevorkyan, EPJ Web of Conferences 138,08004 (2017).

[23] S. Gevorkyan, Recent theoretical calculations of the impact of σ_L on the color transparency.

[24] L. El Fassi et al., Phys. Lett. B 712, 325 (2012).

[25] S. Gevorkyan, V. Jaloyan, A. Kotzinian, Phys. Lett., B 212, 251 (1988).

[26] N. Nikolaev, B. Zakharov, Z.Phys. C49, 607 (1991).

[27] S. R. Gevorkyan, Journal of Physics: Conference series 678,012033 (2016)..

[28] B. Z. Kopeliovich, J. Nemchik, A. Schafer and A. V. Tarasov, Phys. Rev. C **65**, 035201 (2002).

[29] G. F. de Teramond and S. J. Brodsky, Phys. Rev. Lett. **102**, 081601 (2009).

[30] J. R. Forshaw and R. Sandapen, JHEP **1011**, 037 (2010).

[31] J. R. Forshaw and R. Sandapen, Phys. Rev. Lett. **109**, 081601 (2012).

[32] H. Behrend et al., Phys.Rev.Lett. 24,1246 (1970).

[33] J. Abramson et al., Phys.Rev.Lett. 36,1428 (1976).

[34] P. Braccini et al., Nucl.Phys. B24, 173 (1970).

[35] P. Brodbeck et al., Nucl.Phys. B136, 95 (1978).

[36] M. Kotulla et al., Phys. Rev. Lett. 100, 192302 (2008).

[37] M. H. Wood et al., Phys. Rev. Lett. 105, 112301 (2010).

[38] M. Kotulla et al.,Phys. Rev. Lett. 114, 1999903 (2015).

[39] S. Leopold, V. Metag, U. Mosel, Int. J. Mod. Phys. E19, 147 (2010).

[40] T. Tabaru et al. Phys. Rev. C74, 025201 (2006).

[41] The pair spectrometer has been used in the PrimEx experiment and provided the precision on the flux determination better than 1.2%.

[42] M. Williams et al. Phys. Rev. C 80, 065208 (2009).

[43] P. Degtiarenko, A. Fasso, G. Kharashvilli, and A. Somov, Calculation of Radiation Damage to SiPMs in GlueX Experiment, JLAB-TN-11-005, 2011.

[44] P. Degtiarenko, private communications.

[45] M. Staib, GlueX-doc-3357-v5, 2017.